DEVELOPMENT OF COMPUTERIZED WOOD COLOUR SORTING SYSTEM FOR MALAYSIAN WOOD INDUSTRY

LIEW SHAER JIN

FACULTY OF ENGINEERING

UNIVERSITI MALAYA

KUALA LUMPUR

2024

DEVELOPMENT OF COMPUTERIZED WOOD COLOUR SORTING SYSTEM FOR MALAYSIAN WOOD INDUSTRY

LIEW SHAER JIN

DISSERTATION SUBMITTED IN FULFILMENT OF THE REQUIREMENTS FOR THE DEGREE OF MASTER OF ENGINEERING SCIENCE

FACULTY OF ENGINEERING UNIVERSITI MALAYA KUALA LUMPUR

2024

UNIVERSITI MALAYA

ORIGINAL LITERARY WORK DECLARATION

Name of Candidate: Liew Shaer Jin

Matric No: 17079963

Name of Degree: Degree of Master of Engineering Science

Title of Project Paper/Research Report/Dissertation/Thesis ("this Work"):

Development of Computerized Wood Colour Sorting System for Malaysian Wood Industry

Field of Study: Engineering and Engineering Trades

I do solemnly and sincerely declare that:

(1) I am the sole author/writer of this Work;
(2) This Work is original;
(3) Any use of any work in which copyright exists was done by way of fair dealing and for permitted purposes and any excerpt or extract from, or reference to or reproduction of any copyright work has been disclosed expressly and sufficiently and the title of the Work and its authorship have been acknowledged in this Work;
(4) I do not have any actual knowledge nor do I ought reasonably to know that the making of this work constitutes an infringement of any copyright work;
(5) I hereby assign all and every rights in the copyright to this Work to the Universiti Malaya ("UM"), who henceforth shall be owner of the copyright in this Work and that any reproduction or use in any form or by any means whatsoever is prohibited without the written consent of UM having been first had and obtained;
(6) I am fully aware that if in the course of making this Work I have infringed any copyright whether intentionally or otherwise, I may be subject to legal action or any other action as may be determined by UM.

Candidate's Signature   Date:

Subscribed and solemnly declared before,

Witness's Signature   Date:

Name:

Designation:

ABSTRACT

Wood colour sorting is essential in woodworking to maintain uniformity and consistency in the appearance of the final products, thus, improving consumer satisfaction. Majority of the wood manufacturing companies in Malaysia are depending heavily on manual colour sorting that solely relies on human visual inspection, which can be subjective, inconsistent, laborious, and subject to errors. Automation is a goal, however, the cost for implementation of established technologies is always extortionate especially for small and medium industries (SMI). Therefore, the aim of this research is to develop a computerized vision system to perform colour sorting for multi-scale woodworking facilities. To achieve the research goal, our objectives are set to determine a suitable algorithm for colour features classification, to select the best features which contribute the most in the classification and to compare the effect of different cameras in the performance of the colour sorting. We have compared camera of different genres, namely an industrial camera, a prosumer action camera, and a webcam. Three cameras used were: i) Hikrobot® MV-CE200-10UC (CE200), ii) Logitech® C920 HD Pro (C920), and iii) Sony® RX0 II (RX0 II). After setting up a veneer imaging prototype, a total of 1,289 distinct images of American red oak (*Quercus rubra*), yellow poplar (*Liriodendron tulipifera*), and maple (*Acer* spp.) were acquired from each camera, summing up to 3,867 images from all cameras. After performing image preparations and calibrations, 26 features were extracted from each image. The features were based on the average and standard deviation of the wood basal colour and wood grain colour. Salient features were obtained using Sequential Forward Selection (SFS), which were then used to train a Self-Organizing Map (SOM). The results affirmed that the colour of the basal colour is highly correlated with human sorted colour groups. As expected, CE200 performed the best being of industrial grade. Interestingly, C920 exhibited comparable performance to CE200. RX0 II performed the worst due to its interface software

limitations. This proposed system achieved accuracies of 89.0% for red oak, 94.3% for yellow poplar and 96.4% for maple. This research will assist the SMI to develop affordable vision systems for colour sorting.

Keywords: Wood Colour Sorting, Otsu's Threshold, Sequential Forward Selection, Self-Organizing Map

ABSTRAK

Pengisihan warna kayu amat penting dalam industri perkayuan untuk mengekalkan keseragaman dan konsistensi dalam penampilan produk supaya dapat memuaskan pengguna. Majoriti kilang perkayuan di Malaysia masih menggunakan cara manual dalam pengisihan warna kayu yang bergantung pada pemeriksaan manusia yang berkemungkinan subjektif, kurang konsisten dan berlakunya kesilapan. Automasi merupakan cara yang ideal, walau bagaimanapun, kos untuk pelaksanaan teknologi yang sedia ada amat tinggi terutamanya bagi industri kecil dan sederhana. Dengan ini, penyelidikan ini bertujuan untuk membina sistem visual berkomputer untuk melaksanakan pengisihan warna yang fleksibel untuk kilang-kilang perkayuan dengan skala yang berbeza. Untuk mencapai matlamat penyelidikan ini, objektif kami adalah untuk menentukan algoritma yang sesuai untuk klasifikasi ciri-ciri warna, memilih ciri-ciri yang menyumbang kepada prestasi klasifikasi dan membandingkan kesan kamera yang berbeza dalam prestasi pengisihan warna. Kami telah membandingkan kamera dari pelbagai genre, iaitu kamera industri, kamera tindakan prosumer dan kamera web. Tiga kamera yang digunakan ialah: i) Hikrobot® MV-CE200-10UC (CE200), ii) Logitech® C920 HD Pro (C920), dan iii) Sony® RX0 II (RX0 II). 1,289 imej oak merah Amerika (*Quercus rubra*), poplar kuning (*Liriodendron tulipifera*), dan maple (*Acer* spp.) yang dilabelkan oleh pekerja-pekerja kilang telah diambil dengan prototaip pengimejan venir (lapisan kayu nipis) bagi setiap individu kamera, sejumlah 3,867 imej bagi semua kamera. Selepas melakukan penyediaan dan penentukuran imej, 26 ciri-ciri warna telah diekstrak daripada setiap imej. Ciri-ciri tersebut adalah berdasarkan purata dan sisihan piawai bagi warna asas dan ira kayu. Ciri-ciri yang menonjol diperoleh dengan kaedah 'Sequential Forward Selection' (SFS), dan kemudian digunakan untuk melatih mesin klasifikasi 'Self-Organizing Map' (SOM). Keputusan didapati bahawa warna basal berkorelasi dengan kumpulan warna yang diisih manusia. Seperti yang dijangkakan, kamera gred

industri CE200 menunjukkan prestasi yang terbaik. Menariknya, kamera web C920 menunjukkan prestasi yang setanding dengan CE200. Kamera Tindakan RX0 II mempamerkan prestasi yang paling lemah disebabkan oleh batas program kamera. Sistem yang dicadangkan ini telah mencapai ketepatan 89.0% untuk oak merah, 94.3% untuk yellow poplar dan 96.4% untuk maple. Penyelidikan ini akan membantu industri untuk membangunkan sistem visual pengisihan warna yang mampu milik.

ACKNOWLEDGEMENTS

TABLE OF CONTENTS

LIST OF FIGURES

LIST OF TABLES

LIST OF SYMBOLS AND ABBREVIATIONS

1D	:	One-Dimensional
2D	:	Two-Dimensional
3D	:	Three-Dimensional
ANOVA	:	Analysis of Variance
BMU	:	Best Matching Unit
C920	:	Logitech® C920 HD Pro
CE200	:	Hikrobot® MV-CE200-10UC
CIE	:	International Commission on Illumination
CNN	:	Convolutional Neural Network
CRI	:	Colour Rendering Index
HSL	:	Hue, Saturation, and Lightness
HSV	:	Hue, Saturation, and Value
KNN	:	K-Nearest Neighbours
LDA	:	Linear Discriminant Analysis
LED	:	Light Emitting Diodes
MTIB	:	Malaysian Timber Industries Board
MVS	:	Machine Vision System
OSCD	:	Otsu Soft Colour Descriptor
OTV	:	Otsu Thresholding Value
PCA	:	Principal Component Analysis
RGB	:	Red, Green, and Blue
RX0 II	:	Sony® RX0 II
SBS	:	Sequential Backward Selection
SFS	:	Sequential Forward Selection

SIRIM	:	Standards and Industrial Research Institute of Malaysia
SME	:	Small and Medium-Sized Enterprise
SDK	:	Software Development Kit
SOM	:	Self-Organizing Map
SSH	:	Sim Seng Huat Industries Sdn. Bhd.
SVM	:	Support Vector Machine
WM	:	Weng Meng Industries Sdn. Bhd.
μ	:	Mean Value
σ	:	Standard Deviation

CHAPTER 1: INTRODUCTION

1.1   Background

Malaysia is one of the top 5 exporting countries in Asia for wood-based products, such as plywood, furniture, and sawn timber (*Wood Products*, 2021). The performance of Malaysian wood product exports has increased gradually over the past few years, as shown in Figure 1.1. Although there was a performance dip back in 2020 due to the economic impact of the Coronavirus disease 2019 or the COVID-19 pandemic, the wood industry has recovered in the subsequent years, reaching RM 25.213 billion, which accounts for over 15% of the total export value in the year 2022 (*Annual Report*, 2023; *Malaysia External Trade Statistics*, 2022). In short, wood products significantly contribute to Malaysia's export economy, playing a crucial role in international trade.
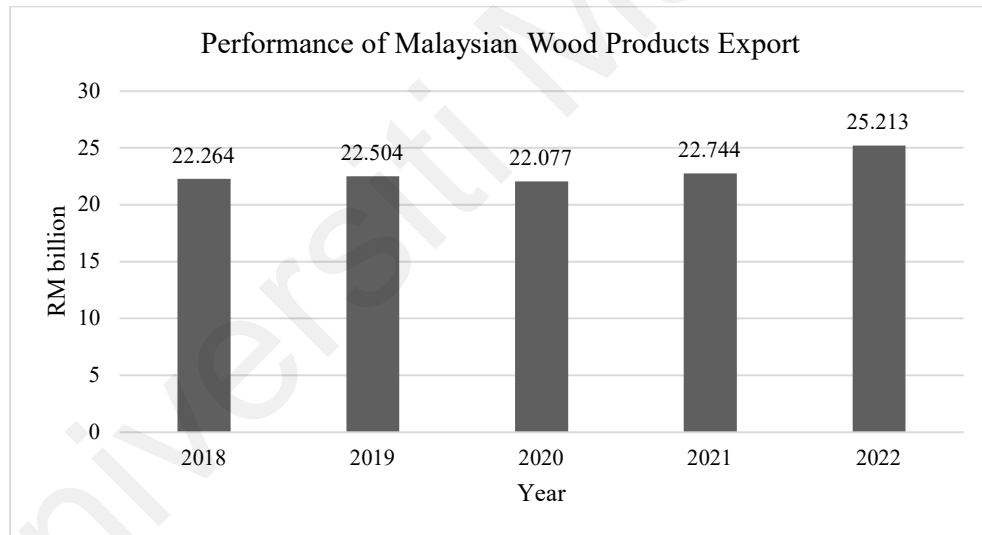
Figure 1.1 Annual performance of Malaysian wood products export from year 2018 to 2022.

Sustainable forestry practices, diversified wood species, and contemporary design aesthetics are among the key determinants that lead to the positive reception and appreciation of Malaysian wood products. Visual aesthetics create pleasure, satisfaction, and quality perception, thus, increasing the market value of wood products. Wood colour homogeneity serves as a vital component in enhancing aesthetic appeal and overall acceptance of wood products (Høibø & Nyrud, 2010; Jonsson et al., 2008). The wood

industry often implements grading systems to categorize and classify wood components to ensure colour consistency of the products meets the consumer satisfaction.

Industries working with wood veneers face different sets of challenges when it comes to colour sorting. Veneers are commonly 0.6 mm thick, but other thicknesses are possible, such as 0.3 mm, 0.5 mm, up to 2.0 mm. They are sliced from a log, or a single piece of timber, therefore veneers in the entire flitch are rather uniform in colour and texture. However, when veneers from different flitches are used, the same problems associated with solid timber pieces apply. While the most logical method of ensuring colour consistency would be to use veneers from the same flitch, however the need for specific lengths for product components, coupled with yield maximization requirements may require veneers from different flitches to be matched together. For instance, the veneers used for the stiles and rails of engineered doors as depicted in Figure 1.2, require colour matching to ensure appearance consistency in the final products.

a)   b)
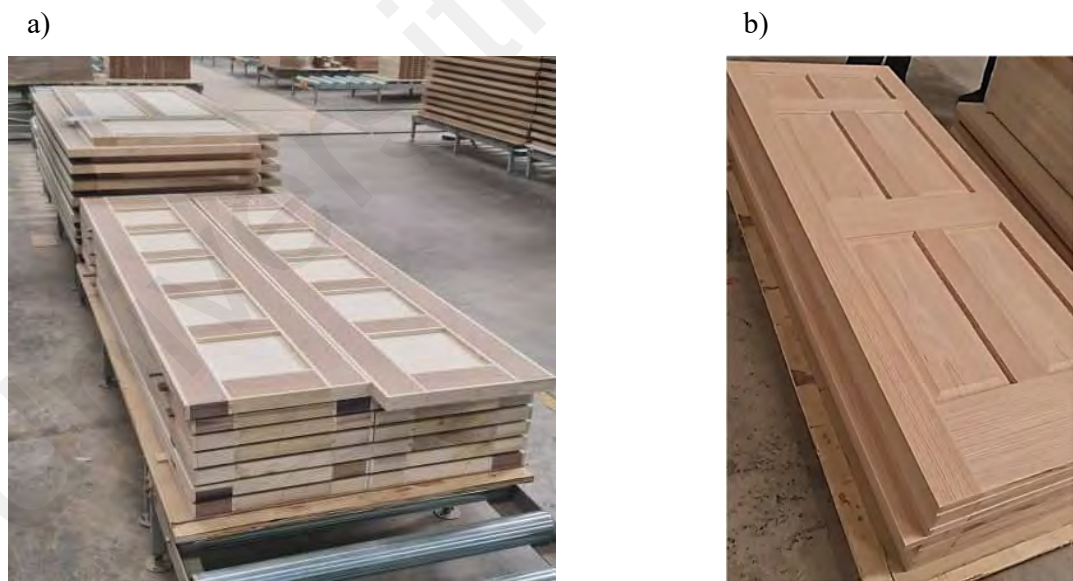
Figure 1.2 Engineered doors a) before veneer lamination and b) after veneer lamination on the stiles and rails.

Manual sorting is the most common method of colour sorting and classification (Wang et al., 2021). This involves human workers manually segregating the wood pieces. There are several techniques employed during segregation – the most common being 'relative judgement' whereby wood components are laid out adjacent to each other and evaluated for colour consistency. Another common approach is to determine the number of colour groups to be sorted to and determining the 'standard bearers' of each group which will be used as reference colour samples.

Human perception of colour difference is nevertheless subjective, inaccurate, and may differ from one observer to another. These inaccuracies may be more pertinent, especially after long hours of such tedious work. The main drawbacks with human inspection include time consumption, fatigue, and lack of concentration (Naqvi, 1996). Visual inspection is therefore vulnerable to human errors (Ramesh et al., 2021). Moreover, most factories rely on natural sunlight as the source of light when performing human colour evaluation, with the option of artificial lighting during overcast days or during night shifts. Since the intensity and colour composition of natural sunlight changes depending on the time of day, weather, cloud conditions, and even position of the sun (or window or door opening) with relation to the timber and observer, getting consistent results is challenging.

Consequently, adopting automated systems not only outperforms human in accuracy, but also has the potential to yield a shorter payback period (Buehlmann & Thomas, 2002). A computerised vision system would be advantageous for an objective and repeatable result. There are several colour sorting machines available in the market as shown in Table 1.1.

Table 1.1 Existing industrial solutions for colour sorting of timber.

Image	Description

	- Company: Michael Weinig AG
	- Model: CombiScan Sense
	- Origin: Germany
	- Functions:
	   o Defect detection (knot/pith/wane/holes/cracks/insect holes)
	   o Unspecified colour sorting for wood pieces

	- Company: WoodEye AB
	- Model: WoodEye Parquet
	- Origin: Sweden
	- Functions:
	   o Defect detection (pith, cracks, holes, sapwood, pitch pocket, darkness, colour, wane, wormhole, structure, angled cracks, knot)
	   o Colour and grain sorting for wood parquet

	- Company: ATB Blank GmbH
	- Model: Spectra for Parquet Sorting
	- Origin: Germany
	- Functions:
	   o Defect detection (pith, cracks, holes, sapwood, pitch pocket, darkness, colour, wane, wormhole, structure, angled cracks, knot)
	   o Colour and grain sorting for wood parquet

	- Company: EBI Electric
	- Model: Inspector B
	- Origin: Canada
	- Functions:
	   o Defect detection (splits, shake)
	   o Colour and grain sorting for known species: American red and white oak, maple, hickory, yellow and white birch, ash, cherry walnut

	- Company: James L. Taylor Manufacturing Company - Model: Opti-Match - Origin: USA - Functions: o Colour sorting of wooded boards into groups of five to seven of best matching pieces

Despite the significance of implementing automated systems and the availability of the technologies, Malaysian wood industry still heavily relies on labour force rather than embracing automated systems (Ratnasingam et al., 2019). Part of the rationale for this could be financial constraints. High initial investment, coupled with a perceived preference for the craftsmanship and flexibility offered by human workers, creates a dynamic where the industry prioritizes the known advantages of a traditional workforce over the potential benefits of automated technologies. Particularly, small and medium-sized enterprises (SMEs) in the wood industry operating within a constrained budget may hesitate when contemplating an investment in costly machinery.

Additionally, concerns about the adaptability and customization to existing procedures may hinder the willingness of most local wood industry players to implement a new automated system. Some of the species targeted by the machines are monospecific timber (European beech, *Fagus sylvatica*; American white oak, *Quercus alba*; American red oak, *Quercus rubra*, etc.), which enables a much simpler colour sorting algorithm to be employed as compared with multi-specific forest species such as red meranti (*Shorea* spp.), which consists of 19 distinct species (Sosef, 2017). The greater the number of species associated with the timber, the larger the variation they will present in terms of its colour, grain density, and overall visual morphology, and all these factors influence the visual properties of the timber.

While challenges may have slowed down the adoption of automated systems, the Malaysian government, on the other hand, actively encouraging the wood industry to embrace Industry 4.0 as technology advances and awareness grows. Initiatives have been undertaken to steer the sector towards a more automated future, addressing challenges and leveraging the advantages of automation to enhance efficiency and competitiveness.

In 2021, the Standards and Industrial Research Institute of Malaysia (SIRIM) and the Malaysian Timber Industry Board (MTIB) signed a Memorandum of Understanding

(MoU) to enhance collaboration. SIRIM, operating under the Ministry of International Trade and Industry (MITI), will partner with MTIB to explore technology areas, including Industry 4.0, machinery and equipment fabrication. Notably, one of the collaborative projects is the development of an automated visual inspection system for assessing wood colour, size, and defects (SIRIM, 2021). This study is funded by the research grant under the project.

1.2   Problem Statement

This research addresses the financial concerns faced by Malaysian wood industries in the investment of an automated vision system for wood colour sorting. By filling the gap in understanding different camera options, the research aims to explore a wider range of imaging equipment in vision system. Besides that, this research targets the system adaptability to diverse wood species. This study seeks to investigate the anticipation of both basal and grain colour attributes in the realm of wood colour characterisation, contributing to a deeper understanding and holding implications for a diverse range of wood species. Additionally, despite the availability of timber colour sorting machines in the market, this research investigates and resolves the challenges of working with delicate veneers, ultimately fostering the development of a wood colour sorting system for veneers.

1.3   Objectives

This research aims to develop a computer vision system for sorting wood products based on colour aspects that align with human visual perception. To achieve this research goal, three main objectives have been identified:

i.   To assess and compare the performance of various camera genres in the context of industrial veneer colour sorting.

ii. To identify and select optimal colour features from the basal and grain aspects that effectively distinguish veneer colour variations in red oak, yellow poplar, and maple.

iii. To deploy an industrial veneer colour sorting prototype

This research holds the potential to advance the development of a highly precise colour sorting mechanism tailored for diverse wood species, with potential applicability to non-tested varieties. The evaluation of camera effectiveness in achieving accurate colour distinctions offers viable options for the industry players, SMEs particularly, who may be grappling with financial limitations. Beyond theoretical exploration, this research aims to translate its findings into practical applications. The deployment of a tangible prototype for industrial veneer colour sorting serves as a testament to the real-world relevance and applicability of the research outcomes, providing valuable insights and solutions for the wood industry.

The research methodology comprises two key processes: image acquisition and image processing. In the image acquisition phase, the hardware system is established, encompassing cameras, lighting, and an enclosure rig. Additionally, software applications are deployed to capture images of the veneer samples. The image processing stage includes essential steps such as pre-processing, features extraction, features selection, and classifier building. The research strives to provide a comprehensive understanding of the

overall system. The findings will elucidate which features contribute most significantly to colour distinguishability. Furthermore, the research explores the impact of various cameras on the performance of the colour sorting process, providing valuable insights into their influence on system outcomes.

1.4   Structure of Dissertation

The dissertation is organized into five chapters, each serving a distinct purpose. The literature review explores past works, laying the foundation for proposed adapted approaches. In the methodology section, the processes are detailed, providing a comprehensive understanding. Results are presented graphically and tabulated, showcasing the findings. Discussions critically compare this study with related work and evaluate the implementation of the first prototype. Finally, the conclusion scrutinizes whether the research goals and objectives are achieved, highlights limitations, and suggests potential avenues for future improvements.

CHAPTER 2: LITERATURE REVIEW

This chapter serves as a foundational exploration into the existing body of knowledge relevant to the essential components of this research. Structured into two main sections, this chapter critically examines the current state of research within the domains of image acquisition and image processing. The image acquisition section reviews key findings related to two pivotal elements: cameras and lighting. Meanwhile, the image processing section analyses the pre-processing approaches, features extraction techniques, feature selection methods and classifiers. This chapter aims to provide a comprehensive understanding of the intricacies involved in both image acquisition and processing, laying the groundwork for the subsequent methodologies and discussions.

2.1   Image Acquisition

A vision system comprises a hardware system designed to capture images for subsequent processing. The quality of the captured images is influenced by the hardware components. The primary hardware components include cameras and lighting systems.

2.1.1   Cameras

The camera serves as the capturing device in a vision system, employing a sensor to transform light information within the field of view into digital signals, resulting in monochrome or colour images. Cameras can be broadly categorized into two types based on imaging techniques: area scan and line scan cameras. As depicted in Figure 2.1, area scan cameras utilize a matrix of pixels arranged in rows and columns, capturing the entire two-dimensional (2D) image in a single exposure. This imaging technique is commonly referred to as 2D imaging. In contrast, line scan cameras have pixels aligned in a linear array along a single axis, capturing images line by line, thus, it is also known as one-dimensional or 1D imaging. The direction of the scan depends on the acquisition setup,

either following the direction of object motion, as seen in conveyor systems, or against the direction of camera motion, as observed in scanner setups.
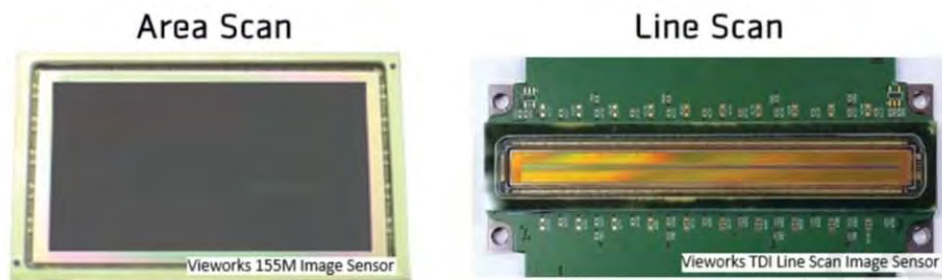
Figure 2.1 Area scan and line scan image sensor (*Line Scan Cameras vs Area Scan Cameras – Which Is Suitable For Your Applications?*).

Table 2.1 outlines the distinct advantage of both area scan and line scan cameras, the choice between them depends on the specific requirements of the application. Line scan cameras excel in high-speed imaging scenarios, such as continuous moving lines like conveyor systems. They can achieve greater resolution since the constructed images are not constrained by fixed vertical resolution, and they require simpler illumination as they scan only a narrower linear area at a time, compared to their area scan counterparts.

In Table 2.2, it is evident that line scan cameras were commonly used to capture wood samples on moving conveyor systems, meeting the industrial requirements of high speed and resolution. The work of Liu and Furuno (2002) achieved a similar output for their images, despite not involving a conveyor system; they utilised a scanner with a moving line scan camera. In contrast to conveyor systems, where vertical resolution can be adjusted based on the length of the object, the vertical resolution in scanners is constrained by the physical size of the device.

On the contrary, area scan cameras are well-suited for applications requiring imaging within a defined scan area. They are cost-effective due to their less complicated installation compared to line scan cameras, which demand precise coordination of

acquisition timing and the motion of the camera or object (Kashyapa, 2021). Generally, they have a more extensive application scope. Table 2.2 demonstrates that area scan cameras exhibit versatility, being applicable in both static systems where wood pieces are placed manually within the camera's field of view, and dynamic systems, where sensors detect the presence of moving wood objects and trigger image capture.

In cases where a single scan cannot accommodate longer pieces, Liu et al. (2020) employed image stitching, capturing images consecutively to reconstruct the entire wood piece. While this approach suited their focus on combining two-colour tones (light and dark) and three different types of textures, it may not be optimal for scenarios requiring the determination of multiple colour groups. Stitching area-scanned images can result in uneven light distribution between seams, potentially misrepresenting colour information and affecting classification performance.

While most researchers utilised a single camera in their work, Srikanteswara et al. (1997) employed two cameras to capture both the top and bottom faces of their wood panels. This choice may be attributed to their emphasis on furniture components, where the selection criteria for panels are typically more rigorous, necessitating both faces to meet similar standards. Conversely, researchers working with wood flooring, joinery or other engineered products concentrated solely on one side of the wood pieces, given that the other side will be covered or hidden. Furthermore, it is often assumed that the colour of a thin wood piece is homogeneous. Consequently, analysing the colour on one side is deemed sufficient to represent the overall colour.

Noteworthily, Nurthohari et al. (2019) implemented a home-office grade webcam in their acquisition system, achieving comparable results with researchers who chose industrial-grade cameras. Given that these studies all employed a single type of camera, an intriguing path for investigation is to study the impact of different camera genres,

ranging from office-grade webcams to industrial cameras, on the performance of colour sorting systems. To address this knowledge gap, the current study compares cameras of three distinct genres: office-grade webcam, action camera, and industrial camera. Considering the wood sample type in this study is confined to wood veneer, the use of an area scan camera with a quasi-dynamic system for industrial setting is deemed most suitable. This could be achieved by deploying a conveyor system for transmission, with pauses for capture under the camera. This choice is driven by the thin and fragile nature of veneers, requiring careful handling.

Table 2.1 Comparison between area scan and line scan cameras.

	Area Scan Camera	Line Scan Camera
Sensor Configuration	Pixels arranged in 2D array	Pixels arranged in 1D array
Working Principle	Capture an image in a single exposure	Capture an image line by line
Resolution	Limited by number of pixels in both horizontal and vertical axes	Limited by number of pixels in the horizontal axis, vertical resolution varied by object length or constrained by camera physical memory
Illumination Area *	Wider	Narrower
Object Motion Coordination	Not critical	Critical to synchronize capture timing with object motion
General Application	Defined scan area, can be employed in both static and dynamic systems	High-speed continuous moving systems like conveyor systems
Cost Effectiveness	Higher for its less complicated setup	Lower for its more complicated installation and fine coordination

* Assuming similar working distance and scan area width

Table 2.2 Acquisition system setups of related work.

Wood Sample Type		Wood Sample State of Motion		Imaging Technique		Camera Position Relative to Sample		Camera Count	Source
Solid	Veneer	Linear Movement	Stationary	Area Scan	Line Scan	Top	Bottom		
✓		✓			✓	✓	✓	2	Lu et al. (1997); Srikanteswara et al. (1997)
✓		✓			✓	✓		1	Bombardier et al. (2008); Wang et al. (2021)
✓		✓			✓			1	Lin et al. (2020)
✓			✓		✓		✓	1	Liu and Furuno (2002)
✓		✓			✓	✓		1	Zhuang et al. (2021)
✓		✓		✓		✓		1	Liu et al. (2020)
✓		✓		✓		✓		1	Nurthohari et al. (2019)
✓			✓	✓		✓		1	Kurdthongmee (2008); Lu and Tan (2004)
✓			✓	✓		✓		1	Bianconi et al. (2013)

2.1.2   Lighting

Luminance is integral to colour perception. In a vision system, maintaining appropriate luminance levels ensures faithful colour reproduction. Moreover, maintaining consistent luminance is important for the reliability of the vision system's analysis. Consistency ensures that the system algorithms can be applied uniformly, regardless of variations in lighting conditions.

Table 2.3 showed the lighting setups of the studies which employed area scan camera. Although light emitting diodes (LEDs) or fluorescence lamps were suitable light sources, LEDs have gain significant popularity over the years due to their proven better energy efficiency more environmentally friendly outcomes (Perdahci et al., 2018). Additionally, LED lights have a higher colour rendering index (CRI) compared to fluorescent lights, which enables them to accurately display a wider range of colours (Heffernan et al., 2007).

There are generally two lighting techniques: direct or indirect lighting. The work of Liu et al. (2020) showcased direct lighting, revealing an uneven lighting illustrated in Figure 2.2. In attempts to minimize this effect, both Nurthohari et al. (2019) and Kurdthongmee (2008) strategically positioned the direct lighting source at a distance, thereby reducing the hotspot created by the light through diffusion. Notably, Nurthohari et al. (2019) achieved optimal performance when the light source was located furthest away from the object.

Figure 2.2 Uneven lighting due to direct lighting (Liu et al., 2020).

Another alternative involves the application of indirect lighting technique such as dome light illumination source adopted by Bianconi et al. (2013). Figure 2.3 shows the arrangement of mounting LEDs upwards facilitates the illumination of the dome from various angles. The dome radiates the light, resulting in the formation of parallel streams of light, ensuring uniform lighting of the target. This technique is especially useful for uneven surface, making it an advantageous choice for scenarios involving of wood veneers.
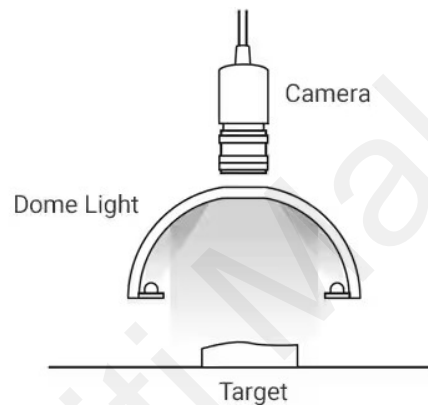
Figure 2.3 Dome light illumination technique (*Dome Lights*).

One of the complications with veneers is that they are typically sliced from green timber or wet logs, and then dried. This causes some sheets of veneers to curl, warp or buckle depending on internal stresses present in the wood fibres. Thus, wavy veneers make imaging using a static camera and direct lighting difficult as the shadows and bright spots causes the camera to register inaccurate information of the actual colour of the veneer (when they are eventually pressed flat when laminated onto a substrate). Figure 2.4 presents a comparison between direct lighting and dome light techniques on wavy veneers. Therefore, findings indicate that, for the purposes of this study, the use of dome light proves to be a superior approach for imaging wood veneers.

a) i)   ii)
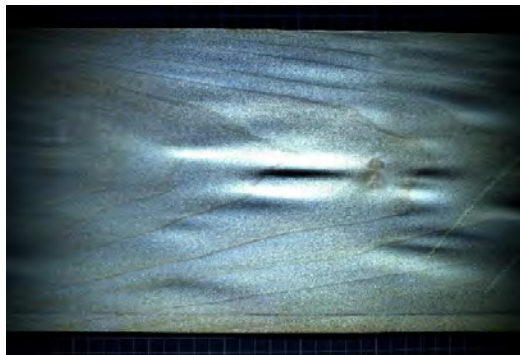
b) i)   ii)
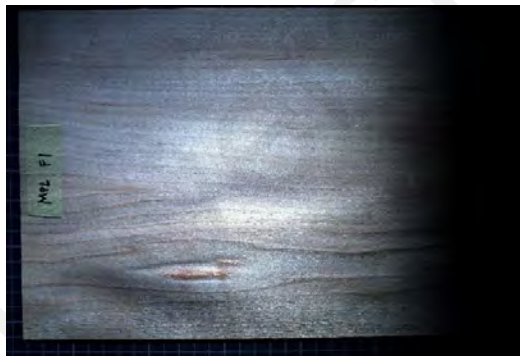
c) i)   ii)

Figure 2.4 Images of the same wavy a) red oak, b) yellow poplar, and c) maple veneers, taken under i) direct lighting (bar light), and ii) a dome light.

Table 2.3 Lightings used in related work.

Light Source	Setup Illustration	Source
LED Panel Light: - Colour Temperature 6500 K - Illuminance 1000 lx		Liu et al. (2020)
Setting 1, LED Strip: - Power 3 W - Illuminance 71 lx - Height 5 cm Setting 2, LED Lamp: - Power 3 W - Illuminance 401 lx - Height 10 cm Setting 3 *, LED Lamp: - Power 6 W - Illuminance 1201 lx - Height 15 cm * Optimal setting		Nurthohari et al. (2019)
LED Dome Light: - Voltage 18 V - Illuminance 78,600 lx		Bianconi et al. (2013)
Fluorescent Lamp: - Power 15 W - Colour Temperature 5000 K - Illuminance 4150 lx - Distance 3 m angled at 45 °	-	Kurdthongmee (2008)

2.2   Image Processing

Image processing is the backbone of a machine vision system, interpreting the visual information in the form of digital images. It involves a series of computational techniques and algorithms applied to digital images to extract meaningful insights, patterns, and features. In the context of automated colour sorting machine, image processing plays a paramount role in tasks ranging from colour feature extraction to classification.

2.2.1   Image Pre-processing

Image pre-processing is a pivotal step in computer vision and image analysis to enhance the quality and interpretability of digital images. This preliminary stage involves a series of operations applied to raw images before they undergo more complex analyses. The primary objective is to address various challenges introduced during image acquisition, such as noise, distortion, and uneven illumination, thus, improving the overall reliability and accuracy of subsequent image analysis tasks, including feature extraction and classification.

Different lightings of the same setting will result in images with different colour profiles. When designing a vision system, it is crucial to possess the insights of the lighting conditions to prevent erroneous interpretations derived from raw images. Dealing with scenarios where lighting conditions may vary, colour calibration will be carried out to rectify the images to ensure consistent intensity levels for identical colours. In Figure 2.5, Sunoj et al. (2018) demonstrated how different lighting conditions affect the image intensities and the correction done with a standard colour calibration chart.
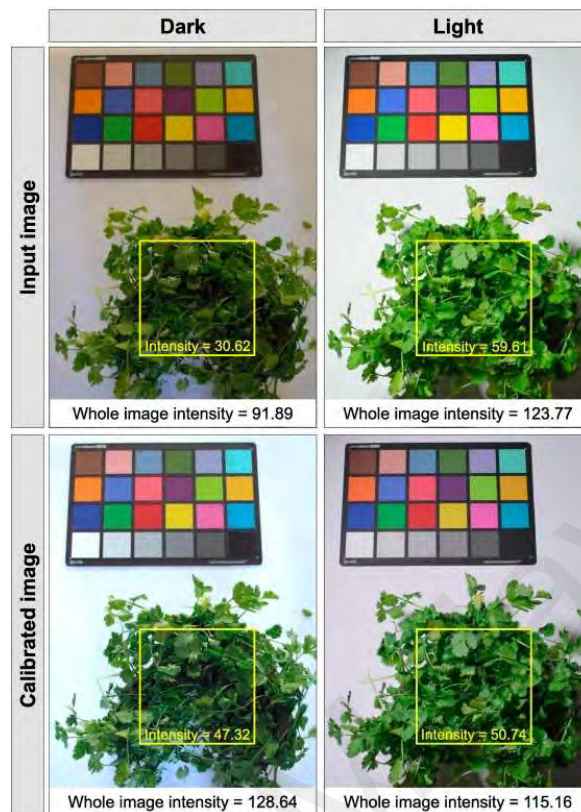
Figure 2.5 Intensities of colour images before and after calibration under two lighting conditions (Sunoj et al., 2018).

McCamy et al. (1976) had introduced the ColorChecker Color Rendition Chart (also called the Macbeth Chart, as utilised in Figure 2.5 and Figure 2.6) with 24 squares of colour samples which reflect light consistently under a variety of lighting conditions over time. The colour chart has become essential as an image calibration tool, especially in photography.

a)   b)   c)
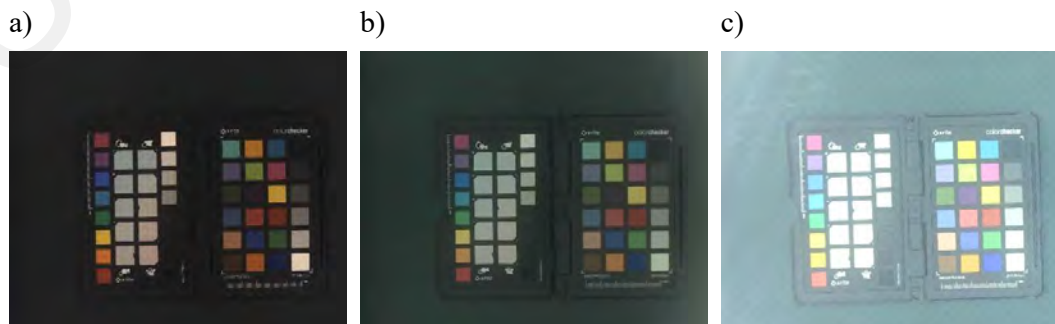
Figure 2.6 Macbeth calibration chart as imaged using a) Hikrobot MV-CE200-10UC, b) Logitech C920 HD Pro webcam, and c) Sony RXO II action camera.

Most studies implemented controlled lighting settings and conducted their image acquisition within specific time frames, the need for colour calibration may not be necessary. This assumption stems from the presumption that the lighting conditions remained constant, or any variations were deemed negligible. However, deterioration can occur over time, particularly in the case of aging lights or camera equipment, especially within the harsh environment of industrial settings. This will inevitably lead to inaccurate results particularly in colour classification tasks (McCamy et al., 1976).

Therefore, it is always a good practice to incorporate calibration into any machine vision system to accommodate variabilities in real life applications particularly for use over long periods of time. This is important for addressing factors like the replacement of cameras or lighting equipment. Periodic calibration is essential to ensure the sustained quality of the colour images, thereby minimizing misclassification rates.

2.2.2 Feature Extraction

Feature extraction is a critical component that bridges raw visual data with meaningful information. As the initial step in the process, feature extraction involves the identification and isolation of relevant characteristics or patterns from digital images of wood samples. The extracted features serve as distinctive markers, enabling the machine vision system to discriminate between different colour tones. This process lays the foundation for subsequent classification algorithms to precisely categorise, and sort wood pieces based on their distinct colour characteristics.

2.2.2.1 Colour Space

Colour space refers to a specific organisation of colours, defining the range and combinations of colours that can be represented. It provides a way to express and quantify colours in a standardized manner. When working with digital images, it is essential to be

aware of the colour space used by the camera and to choose the appropriate colour space for specific output requirements or post-processing tasks.
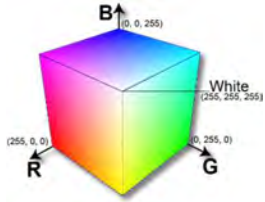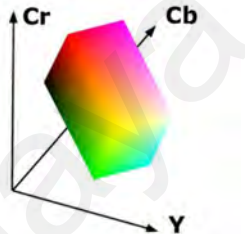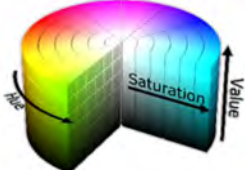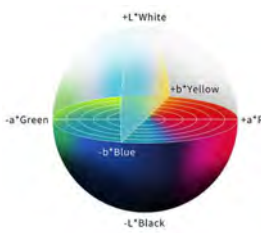
Understand how the image sensor in the camera works helps to comprehend the colour space output from the camera. The sensor incorporates a Bayer filter over its pixels, with each pixel having either a red, green, or blue filter arranged in a mosaic pattern, as shown in Figure 2.7. Each pixel captures only one colour, and interpolation of neighbouring pixel values is employed to estimate the missing colour information to reconstruct a full-colour image. The arrangement includes more green filters as the human eye is more sensitive to green light.
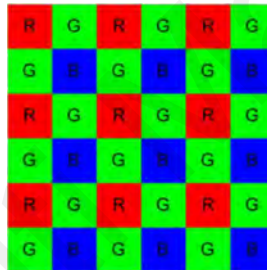
Figure 2.7 Bayer pattern (*Monochrome Camera vs. Color Camera: All You Need to Know*).

As outlined in Table 2.4, colour spaces are graphically represented through coordinate systems, each offering unique characteristics. The RGB colour space utilizes intensities of red, green, and blue ranging from 0 to 255 to define individual pixels. YCbCr colour space employs luminance (Y) in the range of 16 to 235, accompanied by chrominance components (Cb and Cr) ranging from 16 to 240. HSL and HSV colour spaces, although similar, differ in their representation of hue (0° to 360°), saturation, and value or lightness (expressed as percentages). HSL uses a lightness component in percentages, where 100% signifies white, while HSV employs a value component to indicate blackness. The CIEL*a*b* colour space incorporates L* for lightness (0 to 100) and a* and b* for chromaticity, representing green to red and blue to yellow, respectively.

21

Table 2.4 Colour components of different colour spaces.

Colour Space	Colour Components			
RGB	R (Red Intensity)	: 0 – 255		[1]
	G (Green Intensity)	: 0 – 255		
	B (Blue Intensity)	: 0 – 255		
YCbCr	Y (Luminance / Brightness)	: 16 – 235		[2]
	Cb (Blue Chrominance)	: 16 – 240		
	Cr (Red Chrominance)	: 16 – 240		
HSL	H (Hue / Colour Type)	: 0 – 360 °		[3]
	S (Saturation / Colour Intensity)	: 0 – 100 %		
	L (Lightness / Brightness)	: 0 – 100 %		
HSV	H (Hue / Colour Type)	: 0 – 360 °		[3]
	S (Saturation / Colour Intensity)	: 0 – 100 %		
	V (Value / Blackness)	: 0 – 100 %		
CIEL*a*b*	L* (Lightness)	: 0 – 100		[4]
	a* (Green to Red)	: -110 – 110		
	b* (Blue to Yellow)	: -110 – 110		

[1]: *How to Convert an RGB Image to a Grayscale*

[2]: *File:YCbCrColorSpace Perspective.png*

[3]: *File:Color solid comparison hsl hsv cube cylinder cone.png*

[4]: *Color Management: Know about Color Spaces*

Colour spaces serve as different models for representing colours in digital images. Each colour space comes with its unique set of components, and there might be a need for converting between these spaces for specific purposes or to ensure compatibility with different devices and standards. Conversion between colour spaces involves transforming the colour information from one model to another while preserving the perceived visual information. Table 2.5 presents the interrelationships between the widely used RGB colour space and other common colour spaces.

Table 2.5 Conversion table for common colour spaces.

RGB to HSL	HSL to RGB
When R, G and B are integers between 0 and 255:	When $0° \leq H \leq 360°, 0 \leq S \leq 1, 0 \leq L \leq 1$:

RGB to HSL

When R, G and B are integers between 0 and 255:

$$\begin{pmatrix} R' \\ G' \\ B' \end{pmatrix} = \begin{pmatrix} \dfrac{R}{255} \\ \dfrac{G}{255} \\ \dfrac{B}{255} \end{pmatrix}$$

$$C_{max} = \max(R' \quad G' \quad B')$$
$$C_{min} = \min(R' \quad G' \quad B')$$
$$\Delta = C_{max} - C_{min}$$

$$H = \begin{cases} 0°, & \Delta = 0 \\ 60° \times \left(\dfrac{G' - B'}{\Delta} \mod 6\right), & C_{max} = R' \\ 60° \times \left(\dfrac{B' - R'}{\Delta} + 2\right), & C_{max} = G' \\ 60° \times \left(\dfrac{R' - G'}{\Delta} + 4\right), & C_{max} = B' \end{cases}$$

$$S = \begin{cases} 0, \Delta = 0 \\ \dfrac{\Delta}{1 - |2L - 1|}, \Delta \neq 0 \end{cases}$$

$$V = \frac{C_{max} + C_{min}}{2}$$

HSL to RGB

When $0° \leq H \leq 360°, 0 \leq S \leq 1, 0 \leq L \leq 1$:

$$C = (1 - |2L - 1|) \times S$$
$$X = C \times \left(1 - \left|\left(\frac{H}{60}°\right) \mod 2 - 1\right|\right)$$
$$m = L - \frac{C}{2}$$

$$\begin{pmatrix} R' \\ G' \\ B' \end{pmatrix} = \begin{cases} \begin{pmatrix} C \\ X \\ 0 \end{pmatrix}, & 0° \leq H < 60° \\ \begin{pmatrix} X \\ C \\ 0 \end{pmatrix}, & 60° \leq H < 120° \\ \begin{pmatrix} 0 \\ C \\ X \end{pmatrix}, & 120° \leq H < 180° \\ \begin{pmatrix} 0 \\ X \\ C \end{pmatrix}, & 180° \leq H < 120° \\ \begin{pmatrix} X \\ 0 \\ C \end{pmatrix}, & 240° \leq H < 300° \\ \begin{pmatrix} C \\ 0 \\ X \end{pmatrix}, & 300° \leq H < 360° \end{cases}$$

$$\begin{pmatrix} R \\ G \\ B \end{pmatrix} = \begin{pmatrix} (R' + m) \times 255 \\ (G' + m) \times 255 \\ (B' + m) \times 255 \end{pmatrix}$$

RGB to HSV	**HSV to RGB**

When R, G and B are integers between 0 and 255:

$$\begin{pmatrix} R' \\ G' \\ B' \end{pmatrix} = \begin{pmatrix} \dfrac{R}{255} \\ \dfrac{G}{255} \\ \dfrac{B}{255} \end{pmatrix}$$

$C_{max} = \max (R' \quad G' \quad B')$
$C_{min} = \min (R' \quad G' \quad B')$
$\Delta = C_{max} - C_{min}$

$$H = \begin{cases} 0°, & \Delta = 0 \\ 60° \times \left(\dfrac{G' - B'}{\Delta} \bmod 6 \right), & C_{max} = R' \\ 60° \times \left(\dfrac{B' - R'}{\Delta} + 2 \right), & C_{max} = G' \\ 60° \times \left(\dfrac{R' - G'}{\Delta} + 4 \right), & C_{max} = B' \end{cases}$$

$$S = \begin{cases} 0, & C_{max} = 0 \\ \dfrac{\Delta}{C_{max}}, & C_{max} \neq 0 \end{cases}$$

$$L = C_{max}$$

When $0° \leq H \leq 360°, 0 \leq S \leq 1, 0 \leq V \leq 1$:

$C = V \times S$
$X = C \times \left(1 - \left| \left(\dfrac{H}{60}° \right) \bmod 2 - 1 \right| \right)$
$m = V - C$

$$\begin{pmatrix} R' \\ G' \\ B' \end{pmatrix} = \begin{cases} \begin{pmatrix} C \\ X \\ 0 \end{pmatrix}, & 0° \leq H < 60° \\ \begin{pmatrix} X \\ C \\ 0 \end{pmatrix}, & 60° \leq H < 120° \\ \begin{pmatrix} 0 \\ C \\ X \end{pmatrix}, & 120° \leq H < 180° \\ \begin{pmatrix} 0 \\ X \\ C \end{pmatrix}, & 180° \leq H < 120° \\ \begin{pmatrix} X \\ 0 \\ C \end{pmatrix}, & 240° \leq H < 300° \\ \begin{pmatrix} C \\ 0 \\ X \end{pmatrix}, & 300° \leq H < 360° \end{cases}$$

$$\begin{pmatrix} R \\ G \\ B \end{pmatrix} = \begin{pmatrix} (R' + m) \times 255 \\ (G' + m) \times 255 \\ (B' + m) \times 255 \end{pmatrix}$$

RGB to YC$_b$C$_r$ <Hamilton 1992>	**YC$_b$C$_r$ to RGB** <Hamilton 1992>

$Y = 0.299R + 0.587G + 0.114B$
$C_b = -0.1687R - 0.3313G + 0.5B + 128$
$C_r = 0.5R - 0.4187G - 0.0813B + 128$

$R = Y + 1.402(C_r - 128)$
$G = Y - 0.34414(C_b - 128) - 0.71414(C_r - 128)$
$B = Y + 1.772(C_b - 128)$

RGB to CIEXYZ	**CIEXYZ to RGB**

$$\begin{bmatrix} x \\ y \\ z \end{bmatrix} = \begin{bmatrix} 0.4125 & 0.3576 & 0.1804 \\ 0.2127 & 0.7152 & 0.0722 \\ 0.0193 & 0.1192 & 0.9503 \end{bmatrix} \begin{bmatrix} R \\ G \\ B \end{bmatrix}$$

$$\begin{bmatrix} R \\ G \\ B \end{bmatrix} = \begin{bmatrix} 3.2405 & -1.5371 & -0.4985 \\ -0.9693 & 1.8760 & 0.0416 \\ 0.0556 & -0.2040 & 1.0572 \end{bmatrix} \begin{bmatrix} X \\ Y \\ Z \end{bmatrix}$$

CIEXYZ to CIEL*a*b*	**CIEL*a*b* to CIEXYW**

$$\begin{bmatrix} L^* \\ a^* \\ b^* \end{bmatrix} = \begin{bmatrix} 116 f \left(\dfrac{Y}{Y_n} \right) - 16 \\ 500 \left(f \left(\dfrac{X}{X_n} \right) - f \left(\dfrac{Y}{Y_n} \right) \right) \\ 200 \left(f \left(\dfrac{Y}{Y_n} \right) - f \left(\dfrac{Z}{Z_n} \right) \right) \end{bmatrix}$$

where

$t = \dfrac{X}{X_n}, \dfrac{Y}{Y_n}, \text{ or } \dfrac{Z}{Z_n}$
$\delta = \dfrac{6}{29}$
$\begin{bmatrix} X_n \\ Y_n \\ Z_n \end{bmatrix} = $ specified white reference illuminant

$$f(t) = \begin{cases} \sqrt[3]{t}, & \text{if } t > \delta^3 \\ \dfrac{t}{3\delta^2} + \dfrac{4}{29}, & \text{otherwise} \end{cases}$$

$$\begin{bmatrix} X \\ Y \\ Z \end{bmatrix} = \begin{bmatrix} X_n f^{-1} \left(\dfrac{L^* + 16}{116} + \dfrac{a^*}{500} \right) \\ Y_n f^{-1} \left(\dfrac{L^* + 16}{116} \right) \\ Z_n f^{-1} \left(\dfrac{L^* + 16}{116} - \dfrac{b^*}{200} \right) \end{bmatrix}$$

where

$t = \dfrac{X}{X_n}, \dfrac{Y}{Y_n}, \text{ or } \dfrac{Z}{Z_n}$
$\delta = \dfrac{6}{29}$
$\begin{bmatrix} X_n \\ Y_n \\ Z_n \end{bmatrix} = $ specified white reference illuminant

$$f^{-1}(t) = \begin{cases} t^3, & \text{if } t > \delta \\ 3\delta^2 \left(t - \dfrac{4}{29} \right), & \text{otherwise} \end{cases}$$

As summarised in Table 2.6, each colour space has its own strengths and weaknesses, and the choice depends on the specific requirements of the task at hand, such as colour manipulation, image processing, or computer vision applications.

Table 2.6 Advantages and disadvantages of colour spaces used in related work.

Colour Space	Advantages	Disadvantages	Sources
RGB	Intuitive for displays; Common colour space for digital images	May not be perceptually uniform	Kavitha and Suruliandi (2018); Khan et al. (2019); Lin et al. (2020); Liu and Furuno (2002); Manjunath et al. (2001); Singh et al. (2018); Srikanteswara et al. (1997); Zhang et al. (2015)
YCbCr	Separation of brightness and colour information	Not as intuitive for colour manipulation	Hiremath and Bhusnurmath (2016); Hu et al. (2013); Lin et al. (2020); Manjunath et al. (2001)
HSV	Intuitive for selecting colours by human perception	May not be perceptually uniform	Hiremath and Bhusnurmath (2016); Hu et al. (2013); Kurdthongmee (2008); Lin et al. (2020); Manjunath et al. (2001); Wang et al. (2021); Zhuang et al. (2021)
CIEL*a*b*	Perceptually uniform; Suitable for colour corrections	Complex mathematical transformation; Less intuitive	Faria et al. (2008); Hiremath and Bhusnurmath (2016); Kurdthongmee (2008); Musat et al. (2016)

As its effectiveness is as comparable as other colour spaces to perform colour comparisons in machine vision applications, a lot of studies that still preferred RGB colour space since it is the common colour space for digital images and there will be substantial computation overheads to convert RGB colour space to other colour spaces.

2.2.2.2   Colour Feature

Colour features or descriptors play a crucial role in the field of image processing and computer vision, providing the means to quantify and analyse the colour characteristics of digital images. These features serve as invaluable tools, particularly in tasks such as image classification. Colour features or descriptors are derived from the colour components corresponding to the colour space of a digital image. They capture meaningful information about the distribution, intensity and relationships among colours in an image. The following are the common colour features employed in colour classification studies:

(a)   Colour Histogram

A colour histogram represents the distribution of colours in an image, providing a statistical breakdown of the number of pixels with specific colour values. In a histogram, colours are usually grouped into bins, and the height of each bin corresponds to the frequency of pixels with colour values falling within that range. For example, in an RGB image, there are separate histograms for the red, green, and blue colour channels. Colour histograms are easy to implement and require minimal computational load. However, the space, which is a crucial aspect based on the nature of the object used in the study. Moreover, there is a possibility of losing detailed colour information, especially when dealing with samples exhibiting subtle colour variations due to the binning process.

(b)   Colour Percentile

Colour percentile is a statistical measure to describe the relative position of a colour intensity value, providing insights into the distribution of colour intensities across different percentiles of a colour image. This method enables the identification of critical points in the colour spectrum, revealing patterns, concentrations, or variations that may not be apparent through other colour analysis techniques. By assessing colour percentiles,

researchers gain a more comprehensive view of the colour composition and intensity within a colour image, enhancing the precision and depth of their colour-related analyses. Nevertheless, implementing colour percentiles may involve complex calculations and statistical procedures. This complexity arises from the need to organise and analyse a large set of colour data points, which may involve intricate mathematical computations. Additionally, it is essential to handle outliers appropriately as percentile is sensitive to outliers, which could lead to skewed results.

(c) Mean Colour Value (First Moment in Statistics)

The mean value is a fundamental colour feature that provides understanding of the average colour intensity across all pixels in the colour image. In RGB colour space for instance, it is computed by averaging the individual red, green, and blue intensity values of each pixel. The mean represents the central tendency of colour distribution and gives a sense of the overall colour tone of the image. This feature is particularly useful in applications to obtain a general characterization of the dominant colour in a colour image. The mean value is a simple and computationally efficient metric, forming the basis for more advanced colour features and analyses in image processing and computer vision. However, it may not capture nuances in colour variations and may be sensitive to outliers.

(d) Standard Deviation of Colour Values (Second Moment in Statistics)

The standard deviation of the overall colour image is a measure of the amount of variation or dispersion of colour values across each colour component. It quantifies the deviation from each individual pixel colour to the mean colour value. It is computed by calculating the square root of the average of the squared differences between each pixel value and the mean value. A larger standard deviation indicates a greater the degree of colour variability. Conversely, a lower standard deviation suggests more uniformity in colour distribution. This colour feature proves valuable in assessing the overall diversity

or uniformity of colours within an image, shedding light on its complexity or homogeneity. Nonetheless, it is sensitive to outliers and, when used alone, may has limited interpretability and lack detailed information about the specific colour patterns. Thus, it is often complemented with colour mean value for a more comprehensive representation of the overall image.

(e) *Skewness of Colour Values (Third Moment in Statistics)*

Skewness of colour values is a measure of the asymmetry or lack of symmetry in the distribution of colour values within each colour component of an image. It quantifies the degree and direction of deviation from a symmetric distribution. Skewness provides insights into the overall shape and balance of the colour distribution curve. In Figure 2.8, positive skewness indicates that the distribution has a longer right tail, negative skewness suggests a longer left tail, while normal distribution with no skew has equal tails. A positive skewness may signify an abundance of higher-intensity colours, while negative skewness may suggest a prevalence of lower-intensity colours. Calculating skewness involves assessing the third standardized moment of the colour distribution. Despite its capability to reveal distribution characteristics, skewness may be influenced by outliers and should be interpreted in conjunction with other colour features for a thorough understanding of the image.
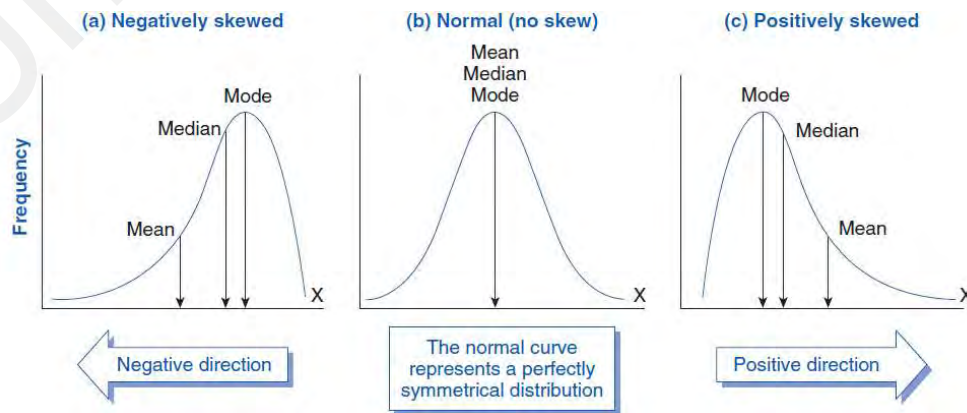
Figure 2.8 Normal versus skewed distribution curves (*Skew*).

(f) ***Kurtosis of Colour Values (Fourth Moment in Statistics)***

Kurtosis of colour values refers to a statistical measure that characterizes the shape of the distribution of colour intensities in an image. It describes the "peakedness" or flatness of a distribution. As illustrated in Figure 2.9, positive kurtosis indicates a distribution with more pronounced and sharper peak, potentially suggesting concentrated colours, while negative kurtosis suggests a flatter distribution with less concentration of colours. Calculating kurtosis involves assessing the fourth standardised moment of the colour intensity distribution. This colour feature aids in understanding the distribution characteristics of colour in an image. However, its sensitivity to outliers and complexity in interpretation have limited its practical utilisation since in most cases, simpler measures like mean and standard deviation might suffice.
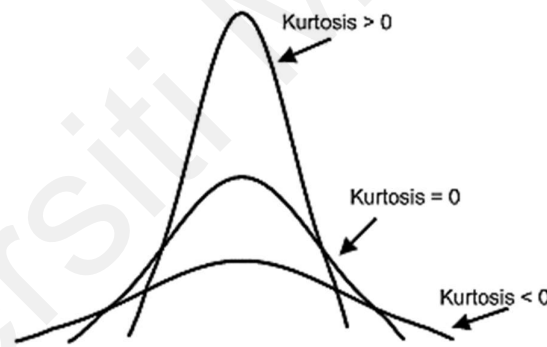
Figure 2.9 Types of kurtosis (*Coefficient of Kurtosis*)

Table 2.7 summarises the commonly used colour features. Histograms provide a statistical breakdown of colour distribution, while percentiles reveal critical points in the colour spectrum. Mean and standard deviation quantify overall colour intensity and variation. Skewness indicates asymmetry in colour distribution, and kurtosis measures the shape of the distribution. Colour features are essential in tasks like colour classification, offering unique insights into the nuances and patterns present in colour images. The choice of features depends on computational load, efficiency, sensitivity to outliers, and the interpretability needed for specific applications.

Table 2.7 Comparison between common colour features in related studies.

	Histogram	Percentile	Mean	Standard Deviation	Skewness	Kurtosis
Formula	$$N = \sum_{i}^{k} m_i$$	$$P = \frac{n}{N} \times 100$$	$$\mu = \frac{\sum_{i}^{N} x_i}{N}$$	$$\sigma = \sqrt{\frac{\sum_{i}^{N}(x_i - \mu)^2}{N}}$$	$$s = \frac{\sum_{i}^{N}(x_i - \mu)^3}{N \times \sigma^3}$$	$$k = \frac{\sum_{i}^{N}(x_i - \mu)^4}{N \times \sigma^4}$$
	N: pixel count k: bin count m_i: bin frequency	P: percentile n: ordinal rank N: pixel count	μ: mean value N: pixel count x_i: pixel value	σ: standard deviation N: pixel count x_i: pixel value μ: mean	s: skewness N: pixel count x_i: pixel value μ: mean σ: standard deviation	k: kurtosis N: pixel count x_i: pixel value μ: mean σ: standard deviation
Computation load	Moderate to high	Moderate	Low	Moderate	Moderate	Moderate
Sensitivity to outliers	Moderate	High	High	High	High	High
Distinguishability of colour nuances	Subtle nuances may be lost due to binning	Critical points in the colour spectrum are captured	Only central point in the colour spectrum is captured	Variations quantified but not captured	Variations could not be captured	Variations could not be captured
Colour information	Colour distribution	Critical colour points	Central colour point	Spread of colours	Symmetricity of distribution	Shape of distribution
Sources	Bianconi et al. (2013); Bombardier and Schmitt (2010); Faria et al. (2008); Kurdthongmee (2008); Lin et al. (2020); Rozman et al. (2006); Srikanteswara et al. (1997); Wang et al. (2021)	Bianconi et al. (2013); Rozman et al. (2006)	Bianconi et al. (2013); Bombardier and Schmitt (2010); Hu et al. (2013); Liu and Furuno (2002); Rozman et al. (2006); Wang et al. (2021); Zhuang et al. (2021)	Bianconi et al. (2013); Hu et al. (2013); Rozman et al. (2006); Wang et al. (2021); Zhuang et al. (2021)	Bianconi et al. (2013); Rozman et al. (2006)	Rozman et al. (2006)

Building on insights from the literature review, where existing studies primarily analyse wood images as a whole or by distinct regions, this study introduces a novel perspective. This study aims to assess the individual contributions of the basal and grain parts to the separability of wood colours. Specifically, this study investigates whether the basal or grain components play a more decisive role in determining overall colour tone. To distinguish between relatively darker grain and brighter basal parts, the widely used Otsu method was leveraged for background-foreground separation. The Otsu method assumes a bipolar distribution, iteratively searching the optimal threshold point until the point where the means of the two groups are maximized. By applying Otsu thresholding in this context, the grain (background) and basal (foreground) parts of the wood can be separated effectively. Subsequently, colour extraction techniques, such as mean estimation, will be applied to these distinct zones for a more nuanced analysis.

2.2.3   Feature Selection

Feature selection involves choosing a subset of relevant features from the original set of features to reduce the model complexity and improve the performance of the following classification. Feature selection aims to retain the most informative and discriminative features while eliminating the irrelevant or redundant ones. This process not only enhances the efficiency of the model but also helps mitigate the risk of overfitting and improves interpretability. Selecting appropriate colour features is vital for accurately representing colours and effectively distinguishing between different colour groups. There are two main types of feature selection: supervised and unsupervised (Kuhn & Johnson, 2013).

2.2.3.1 Supervised Feature Selection

Supervised feature selection methods utilize the target variable (label) during the selection process. This category includes three subtypes: filter method, wrapper method, and intrinsic method.

(a) Filter Method

Filter methods evaluate the relevance of features independently of the chosen machine learning model. They rely on statistical measures to rank or score each feature, dropping features according to their correlation with the labelled output. Common filter methods include Fisher score, chi-squared test, information gain, correlation, analysis of variance (ANOVA), etc. This approach is computationally efficient, model-agnostic, and suitable for high-dimensional datasets. However, feature dependencies and interactions may be overlooked.

(b) Wrapper Method

Wrapper methods select features based on the performance of a specific machine learning model or classifier. They involve iterating through feature subsets and evaluating model performance. Common wrapper methods include sequential forward selection (SFS), sequential backward selection (SBS), etc. This approach starts with either an empty feature set or all features set, using a classifier model to rank the performance of each feature iteratively to include relevant features or eliminate redundant features accordingly. This model-specific method may improve model performance by considering feature interactions. Nevertheless, it is computationally expensive and prone to overfitting.

(c) Intrinsic Method

Intrinsic methods incorporate feature selection within the learning algorithm itself. The model is designed to inherently select relevant features during training. For example,

decision trees and random forests inherently perform feature selection by selecting split points based on feature importance. Features are selected during the model training process based on their contribution to minimizing impurity or maximizing information gain. Integration with the learning algorithm makes it more efficient, although it may not always generalize well, and it is model-dependent.

2.2.3.2 Unsupervised Feature Selection

Unsupervised feature selection methods do not use the target variable during the selection process. They are often used for dimensionality reduction or preprocessing. Unsupervised feature selection methods aim to identify and retain the most relevant features without utilizing information from the target variable. These techniques are particularly useful for tasks where the target variable is unavailable or for dimensionality reduction in high-dimensional datasets. Common unsupervised feature selection methods include principal component analysis (PCA) and autoencoders. Unsupervised feature selection is valuable in scenarios where labelled data is scarce or absent. These methods can help reduce the computational burden associated with training models on high-dimensional data while preserving the intrinsic structure and patterns within the dataset.

Table 2.8 summarizes the approaches to feature selection along with their pros and cons. It is essential to consider the specific characteristics of the data and the goals of the analysis when choosing between supervised and unsupervised feature selection methods.

Table 2.8 Comparison of various feature selection approaches.

		Examples	Advantages	Disadvantages
Supervised feature selection	**Filter method**	Fisher score; Chi-squared test; Information gain; Correlation; ANOVA	Efficient; Model-agnostic; Suitable for high-dimensional datasets	Feature dependencies and interactions may not be considered
	Wrapper method	SFS; SBS	Feature interactions are considered	High computational costs; Prone to overfitting
	Intrinsic method	-	Efficient	Model-dependent
Unsupervised feature selection		PCA; Autoencoders	Labelled data not required; Suitable for exploratory analysis; Effective in handling high-dimensional datasets	Limited interpretability; Validation can be challenging

2.2.4   Classifier

A classifier is a model or algorithm that can automatically assign predefined classes to new, unseen data point based on the patterns identified in the learning process. In the context of wood colour sorting, colour features are the distinctive attributes used by a classifier to distinguish between different colour groups. In this section, common classifiers adapted in the wood colour sorting studies are discussed and compared.

2.2.4.1   K-Nearest Neighbours

K-Nearest Neighbours (KNN) is a type of instance-based learning, where the model makes predictions based on the majority class of its k-nearest neighbours in the feature space. It utilises distance metric, such as Euclidean distance or Manhattan distance, to determine the proximity between data points in the feature space. The parameter k represents the number of neighbours to be considered when making predictions. KNN is simple and intuitive, requires no training phase as the model directly uses the training data during prediction. Nonetheless, it is sensitive to irrelevant or redundant features and, the computational cost rises as the feature set gets larger, where more distance calculations are required for each prediction. Additionally, the choice of k can impact the results; too small a value can lead to overfitting, while too large a value can result in underfitting.

2.2.4.2   Fuzzy Classifier

A fuzzy classifier leverages fuzzy logic to handle uncertainty in data. Unlike conventional classifiers that assign data points to distinct classes, fuzzy classifier assigns each data point to membership values for each class ranging from 0 to 1 using appropriate membership functions. Membership functions map input features to a membership value that indicates the strength of association with a given class. The membership values are then combined with fuzzy rules to decide the class to assign. Fuzzy classifiers excel in

scenarios where the boundaries between classes are vague, or instances exhibit characteristics of multiple classes. However, designing and fine-tuning the fuzzy rules and membership functions can be complex and require domain expertise. Moreover, the degree of membership might be challenging to be interpreted intuitively.

2.2.4.3   Linear Discriminant Analysis

Linear discriminant analysis (LDA) is a statistical method used to discover linear combinations of features that effectively discriminate between classes in a dataset. The primary objective of LDA is to maximize the separation between the means of different classes while minimizing the within-class variance. It achieves this by projecting the feature sets into a new subspace defined by the eigenvectors and eigenvalues derived from the mean vectors and scatter matrices. When classifying new data points, LDA assigns them to the classes with the closest mean in the derived subspace. LDA helps reducing the dimensionality of the feature space while preserving class discriminatory information. Nevertheless, it is sensitive to outliers and assuming that the feature sets are normally distributed.

2.2.4.4   Support Vector Machine

Support vector machine (SVM) is a supervised machine learning algorithm that uses hyperplane in a high-dimensional space to separate data points into different classes. In a two-dimensional space, the hyperplane is a line. In a three-dimensional space, the hyperplane is a plane, and so on. Support vectors are the data points that are closest to the hyperplane and have a crucial role in determining the positioning and orientation of the hyperplane. The aim of SVM is to formulate a hyperplane that maximizes the separation between classes. In cases where classes are not linearly separable, input features can be transformed into a higher-dimensional space, without needing to explicitly calculate the transformed feature vectors, by using kernels include Polynomial, Radial Basis Function,

and Sigmoid. SVM is effective and robust against overfitting in high-dimensional spaces. Despite that, it could be computationally expensive for large datasets and is sensitive to the choice of kernel and parameters.

2.2.4.5 Convolutional Neural Network

A Convolutional Neural Network (CNN) is a class of deep neural networks, leveraging convolutional layers to automatically learn hierarchical representations. CNNs are built of convolutional layers that convolves across the input image to capture local patterns and features, pooling layers to down-sample the spatial dimensions of the feature space and activation functions to introduce non-linearity to the model. CNNs are trained using backpropagation and optimization algorithms like stochastic gradient descent. During training, the model adjusts its parameters (weights and biases) to minimize the difference between predicted and actual outputs. A loss function such as cross-entropy loss is used to measure the difference between the predicted and true labels. CNNs can automatically learn hierarchical representations from data to identify relevant features and have consistently achieved state-of-the-art performance in image classification tasks. Nevertheless, training CNNs can be computationally intensive, requiring powerful hardware, and may require substantial amounts of labelled data for effective training.

2.2.4.6 Self-Organising Map

Self-Organizing Map (SOM) is introduced by Teuvo Kohonen in the 1980s, also known as a Kohonen map, is an unsupervised machine learning algorithm used for clustering and visualizing high-dimensional data. A SOM consists of a grid of nodes or neurons, each represents a weight vector of the same dimensionality as the feature set. The weights are initialized randomly and adjusted its weights based on the input data throughout the training process. The neuron with the weight vector closest to the input is considered the winner or "best matching unit" (BMU). The weights of the BMU and its

neighbours are adjusted to move closer to the input sample. The training process continues for a specified number of iterations or until convergence. Over time, the SOM becomes a topological representation of the input data. After training, the SOM provides a low-dimensional representation of the input data. New input samples are mapped to closest regions to decide the clusters or groups they belong to. SOM is effective for clustering and visualizing high-dimensional data and provides insights into the structure and organization of complex data. However, it is sensitive to hyperparameters and initialization, while the selection of network size and topology may require some trial and error.

The classifiers of related work are tabulated in Table 2.9. Classifiers play a critical role in identification and differentiation of patterns within datasets. Supervised classification methods include techniques like KNN and SVM, where the algorithm learns from labelled training data to make predictions on new, unseen instances. Unsupervised methods, such as clustering algorithms like SOM, group similar data points without predefined class labels. Each classification approach comes with its own set of strengths and weaknesses, making the selection of the most suitable method contingent on the specific characteristics of the dataset and the goals of the analysis.

Table 2.9 Classifiers adapted in related work.

	KNN	Fuzzy Classifier	LDA	SVM	CNN	SOM
Principle	Predict new data based on the majority class of its k-nearest neighbours	Predict new data by using membership values and fuzzy rules	Predict new data based on the class with the closest mean in new subspace	Predict new data based on the region separated by hyperplane	Predict data based on the output from convolutional layers with trained weights	Predict data based on the best matching unit in the trained map
Advantages	Simple and intuitive; Training not required	Suitable for vague class boundaries; Suitable for data with characteristics of multiple classes	Simple; Reducing the dimensionality of the feature space	Effective and robust against overfitting in high-dimensional spaces	Automatically identify relevant features; State-of-the-art approach	Effective for clustering; Visualization of high-dimensional and complex data
Disadvantages	Sensitive to redundant features; High computational cost for large dataset; Sensitive to the choice of k	Domain expertise required in designing the rules and functions; Non-intuitive for interpretation	Sensitive to outliers; Dataset is assumed to be normally distributed	High computational cost for large dataset; Sensitive to the choice of kernel and parameters	Computational intensive; Substantial amounts of labelled data required	Sensitive to hyperparameters and initialization; Trial and error required for selection of network size and topology
Sources	Lin et al. (2020); Lu et al. (1997)	Bombardier and Schmitt (2010); Zhuang et al. (2021)	Hiremath and Bhusnurmath (2016, 2017); Zhang et al. (2015)	Eshaq et al. (2020)	Nurthohari et al. (2019)	Kurdthongmee (2008)

2.3   Summary

This literature review meticulously delineates the principal methodologies and algorithms employed in the pivotal phases of image acquisition and processing, providing a solid groundwork for comprehensive exploration. The exploration of image acquisition in wood colour sorting involves the use of line scan and area scan cameras, tailored to different settings based on the conveyor line speed. Given the fragile nature of wood veneer, an area scan camera with a slow-moving conveyor system is deemed most suitable. The study delves into the comparison of three genres of area scan cameras—industrial grade, action camera, and webcam—to assess their impact on system performance. If the image quality has insignificant effect in the system performance, it would encourage wider adoption of such vision system in the industry.

Controlled lighting is crucial for precise colour image analysis. The review delves into different lighting techniques, emphasizing the discovery of indirect lighting method, like dome light technologies. This approach helps alleviate issues related to uneven lighting and shadows on wavy veneers induced by direct lighting. In the pre-processing stage, calibration emerges as a crucial step, especially in real-life industrial settings where equipment deterioration can affect colour consistency over time. While not always necessary in short-term controlled experiments, calibration becomes essential for long-term industrial applications.

The feature extraction review involves discussions on different colour spaces and colour features. The RGB format is widely adopted for its simplicity and minimal computational load. This study focuses on simpler yet effective features like mean and standard deviation, specifically exploring the separation of grain and basal parts. Understanding the role of grain and basal parts in colour distinguishability is one of the key objectives. The review delves into various supervised and unsupervised feature

selection approaches, identifying the SFS wrapper method as suitable for evaluating the relevance of different features.

The literature presents an array of common classifiers, each with varying intuition and visualisation. The ultimate objective of the study, which involves deploying an industrial prototype, leans towards a visually intuitive approach for enhanced user experience and easier comprehension. The Self-Organizing Map (SOM) stands out as a tool providing visual representations of distinct clusters, effectively conveying the concepts of training and testing. This approach allows for future algorithm expansion to be more inclusive of factory workers. In summary, the comprehensive exploration of current solutions enhances the strategic planning and execution of the methodology in this study.

CHAPTER 3: METHODOLOGY

This chapter outlines the systematic approach employed in the two main phases of the study: image acquisition and image processing. The flowchart depicted in Figure 3.1 provides a visual representation of the integrated process. The methodology initiates with the setup of hardware and software and sample preparation for image acquisition, followed by a series of sequential processing steps encompassing pre-processing, feature extraction, feature selection, and classifier building. Each step is designed to contribute towards the objective of implementing a functional wood colour sorting system.
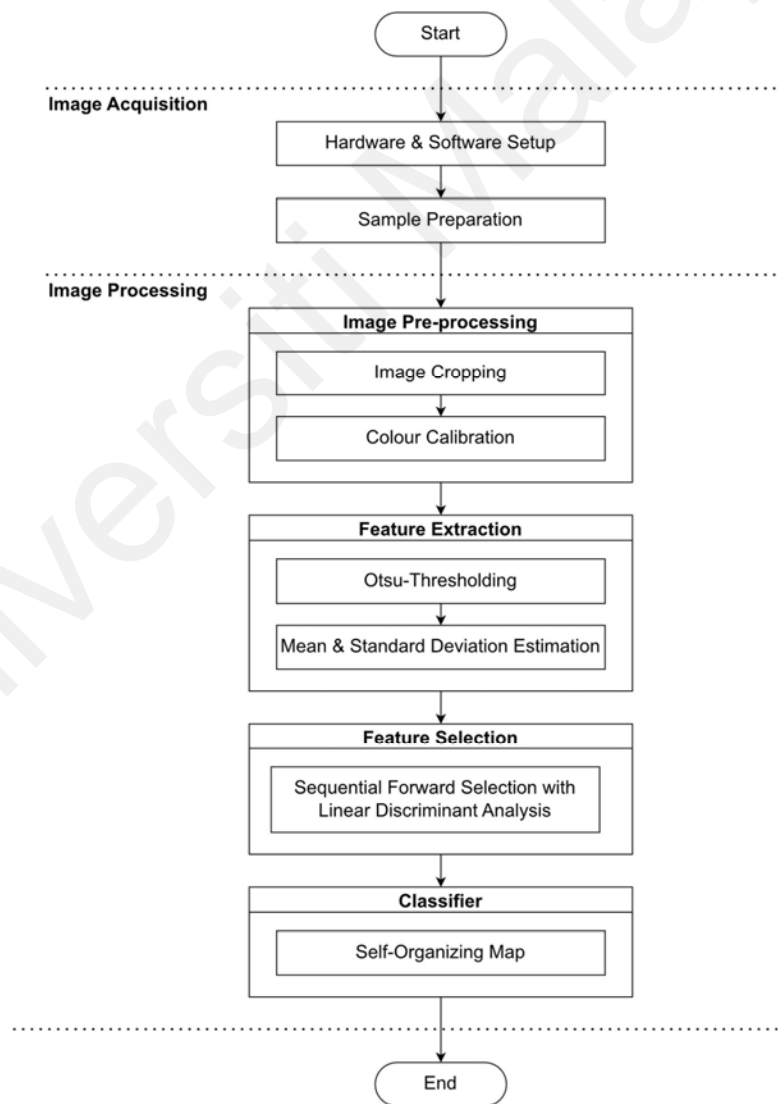
Figure 3.1 Methodology flowchart.

3.1 Image Acquisition

In this section, an overview of the hardware and software setup designed for the acquisition of colour images of wood veneers is presented. The hardware configuration involves detailing the specifications of the chosen cameras and lighting. For the software components, the image acquisition software and camera parameter settings are highlighted.

3.1.1 Hardware Setup

In Figure 3.2, both a 3D rendered image and an actual photograph of the colour sorting machine are presented. The machine is equipped with a versatile conveyor system designed for both manual and auto modes of operation. The inclusion of switches allows for the manual feeding of wood veneers into the image acquisition chamber, while integrated proximity sensors facilitate automated control over the feeding process.

a) 3D rendered image   b) Actual photograph

Figure 3.2 a) 3D rendered image and b) actual photograph of the colour sorting machine.

The close-up of the image acquisition chamber shown in Figure 3.3 reveals the lighting source and cameras. To address the challenges posed by the wavy structure of wood veneers, which is susceptible to shadowing effects, an indirect lighting source is employed. Specifically, a flat dome light, CCS LFXV-300SW, featuring a 300 x 300 mm

illuminating surface area and white light LED with a 5500 K colour temperature, is positioned at the bottom of the chassis, elevated 28 mm above the conveyor belt. This design choice, with a thin case, effectively reproduces the effect of a dome light when used in proximity to the workpiece. Importantly, this innovative solution results in a compact and space-saving system, a departure from the conventional bulkier dome light configurations typically needed for the required illuminating surface area.

Cameras from three common genres with different price range and resolution were selected for comparison: lower-tier webcam, mid-tier action camera and higher-tier industrial camera. For instance, Logitech C920 HD Pro webcam (C920) of 3.0 megapixels, Sony RX0 II action camera (RX0 II) of 15.3 megapixels, and Hikrobot MV-CE200-10UC industrial camera (CE200) of 20.0 megapixels were selected to represent each of the genres of cameras mentioned. The cameras were placed on the top center of the chassis, arranged inline along the moving direction of the conveyor belt. The centers of the lens were 80 mm apart and the front tip of the lens were 280 mm above the conveyor. The industrial camera with narrower field of view was positioned in the middle with the other two cameras on either side of it.
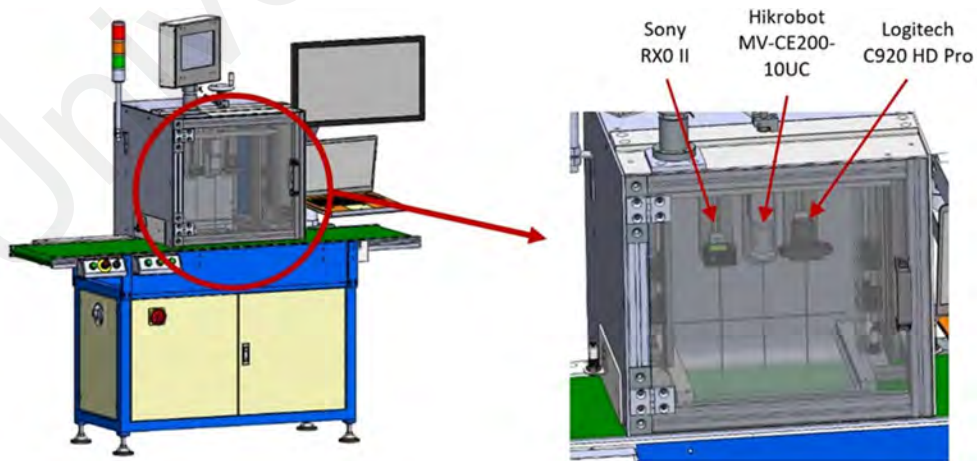
Figure 3.3 Close-up of the image acquisition chamber.

3.1.2   Software Setup

The software used for image acquisition for CE200, RX0 II and C920 are Machine Vision Software MVS V3.3.1 by Hangzhou Hikrobot Technology Co., Ltd., Image Edge Desktop by Sony Corporation and MATLAB R2021b by MathWorks respectively. When using MVS software and MATLAB to connect to CE200 and C920, image acquisition properties such as pixel format, resolution, gain, focus, exposure and white balance can be customised. However, when using Image Edge Desktop, these parameters are preset and cannot be changed.   Table 3.1 in the following summarises the parameters of the cameras used.

Table 3.1 Camera parameters for image acquisition.

Parameters	Cameras		
	CE200	**RX0 II**	**C920**
Image Format	Bitmap	Jpeg	Bitmap
Pixel Format	RGB	RGB	RGB
Bit Depth	24	24	24
Resolution	5472×3648	5472×3648	1920×1080
Gain	Disabled	Not shown	Not shown
Focus	Manual	Auto	Manual
Exposure Mode	Manual	Auto	Manual
White Balance	Manual	Auto	Manual
Gamma Correction	None	Yes	Yes

3.1.3 Sample Preparation

Veneer samples supplied by Weng Meng Industries Sdn. Bhd. (WM) were pre-sorted manually into different colour groups and labelled by the factory personnels. Veneers are restocked upon request from customer orders. Veneer images acquisition was carried out on six non-consecutive dates over a period of two months (Mar to May 2022) to include samples from different batches to account for intragroup variability. Prior to each session of image acquisition, images of the X-rite ColorChecker Passport Photo 2 (ColorChecker) were captured with each camera as the colour reference for the calibration in the later stage of image processing. A total of 1,289 distinct images of veneers from red oak, yellow poplar and maple were obtained with each camera, summing up to 3,867 images taken by the three cameras. The breakdown of the image count by colour groups is tabulated in Table 3.2.

Table 3.2: Veneer image count per camera, broken down by human-classified colour groups*, for red oak, yellow poplar, and maple.

Date	Red Oak				Yellow Poplar			Maple		
	D	O	W	Y	D	W	Y	R	W	Y
10/3/2022	0	14	0	43	11	39	22	0	0	0
21/3/2022	0	0	0	0	27	26	20	0	0	0
31/3/2022	64	42	37	37	37	62	46	67	60	0
20/4/2022	50	59	50	76	0	0	0	63	47	47
28/4/2022	46	0	0	0	0	0	0	0	0	51
12/5/2022	0	0	0	0	40	0	46	0	0	63
Subtotal	**160**	**115**	**87**	**153**	**115**	**127**	**134**	**130**	**107**	**161**
Total	**515**				**376**			**398**		

* D = Dark, O = Orange, Y = Yellow, W = White

3.2 Image Processing

All the analysis were performed using MATLAB R2022a on two PCs with the following specifications: i) Intel® Core™ i7-9700 CPU with 16 GB RAM, and ii) Intel® Core™ i7-11700 CPU with 16 GB RAM. For actual implementation, the MATLAB functions were translated into Visual Basics language, in which the system software program was written.

3.2.1 Image Pre-processing

Images were enhanced in preparation steps to facilitate the feature extraction. Image preparation involved two steps: background removal and colour calibration. In background removal, the images were cropped and masked. Cropping was done to the boundaries around the overlapping region of the field of view of the three cameras. The boundaries were indicated by manually comparing the relative position of the images with a measuring tape. Any blurred edges due to the feathering effect around the lighting frame were excluded from the cropped region.

After image cropping, the remaining of the images may contain unwanted background i.e., regions with conveyor when the incoming veneer pieces were narrow in width. Background removal process was done with the moving average gradient analysis process with the following steps:

1. Filter image with 3-by-3 Gaussian kernel: $\frac{1}{16} \times \begin{bmatrix} 1 & 2 & 1 \\ 2 & 4 & 2 \\ 1 & 2 & 1 \end{bmatrix}$

2. Apply 50 data-point moving average filter to the red intensities of vertical slices with n pixels each, where the averaged red value at any y position, $r_y =$

$$\begin{cases} \sum_{i=1}^{y+24} \frac{r_i}{y+24} \,, \; y \le 25 \\ \sum_{i=y-25}^{y+24} \frac{r_i}{50} \,, 25 < y < n-23 \\ \sum_{i=y-2}^{n} \frac{r_i}{n-y+26} \,, \; y \ge n-23 \end{cases}$$

3. Find the gradient of the average curve in Step 2 by computing the difference between two consecutive pixels.

4. Locate the maximum peak and minimum peak of the gradient curve in Step 3.

5. Top-justify the image to the furthest maximum peak from top.

6. Mask the pixels below the minimum peaks by setting R, G and B values zero.

The process is visualised in Figure 3.4.
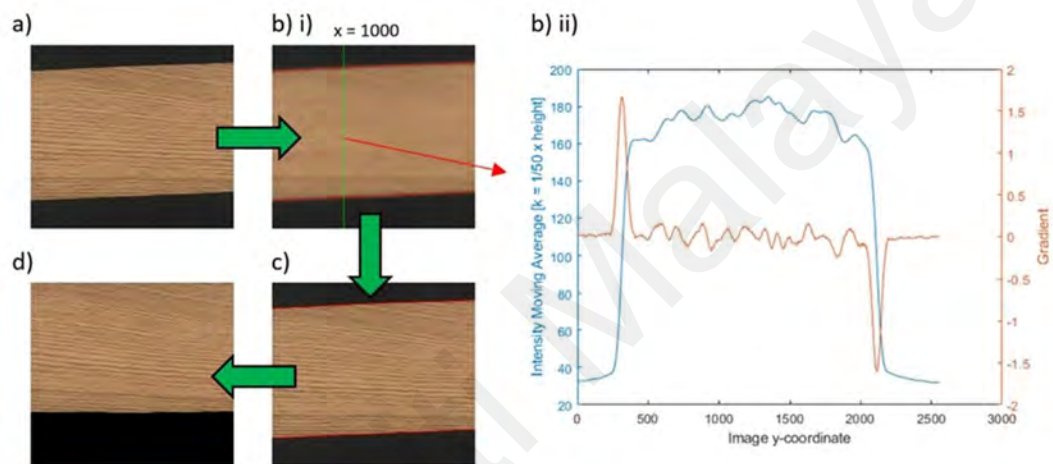
Figure 3.4 The flow of moving average gradient analysis process: a) cropped image, b) i) gaussian filtered image, example of a slice at x=1000 highlighted in green, b) ii) slice analysis plot, blue curve - moving average of red intensities, red curve - gradient curve. c) peaks of each slice highlighted in red. d) image top justified and the region below the bottom red line is masked.

The output images from background removal process then underwent the calibration process. The calibration was done with the images of ColorChecker taken before each session of image capturing. The image of the first day was used as the reference where all others were correlated to. There was no correction done on the images taken on the first day. For all other days, the R, G and B values of all 24 standard reference points were compared to the target image to obtain the average drift values. The deviation values were used in the adjustment on the images captured on the same day.

The output images of RX0 II and C920 are gamma corrected by the camera processor to closely correspond to the non-linear light intensity response curve in human vision. CE200 camera however produces images with linear response curve, thus, those images were gamma corrected as shown in Figure 3.5 a) with a ɣ value of 1/2.2 to better emulate how human perceives light. The corrected image of CE200 day 1 calibration chart was then used as the reference to adjust brightness plots of images from other days for all cameras with an assumption that the shifts are linear.
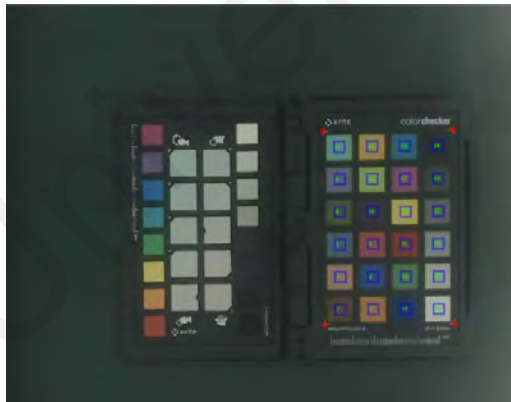
a) i)

a) ii)

b)

c)

Figure 3.5 Day 1 calibration charts of a) CE200 i) before and ii) after gamma adjustment, b) C920, and c) RX0 II.

3.2.2 Feature Extraction

The features were extracted with Otsu thresholding approach as the Otsu Soft Colour Descriptors (OSCD) with the following steps:

1. Compute the histogram of the input grayscale image for intensity level ranged from 0 to 255.

2. Normalize the histogram by dividing each bin by the total number of pixels: $P(i) = \frac{h(i)}{N}$, where $P(i)$ normalized probability of intensity level $h(i)$ is the histogram value at intensity level i, and N is the total number of pixels.

3. Compute the cumulative probabilities: $P_r(i) = \sum_{k=0}^{i} P(k)$, where $P_r(i)$ is the cumulative probability of intensity level i.

4. Compute the cumulative mean: $\mu_r(i) = \sum_{k=0}^{i} k \cdot P(k)$, where $\mu_r(i)$ is the cumulative mean of intensity level i.

5. Compute global mean: $\mu_T = \sum_{k=0}^{255} k \cdot P(k)$.

6. Calculate the between-class variance for each intensity level: $\sigma_B{}^2(i) = \frac{[\mu_T \cdot P_r(i) - \mu_r(i)]^2}{P_r(i) \cdot (1 - P_r(i))}$, where $\sigma_B{}^2(i)$ is the between-class variance at intensity level i.

7. Find the optimal threshold that maximises the between-class variance, $Threshold = \arg max_i \sigma_B{}^2(i)$.

8. Create bit masks for lower stratum and upper stratum based on the threshold value.

9. Apply the masks onto the pre-processed image individually.

10. Estimate the mean and standard deviation of each channel for both strata.

The masking of a pre-processed image is illustrated in Figure 3.6.
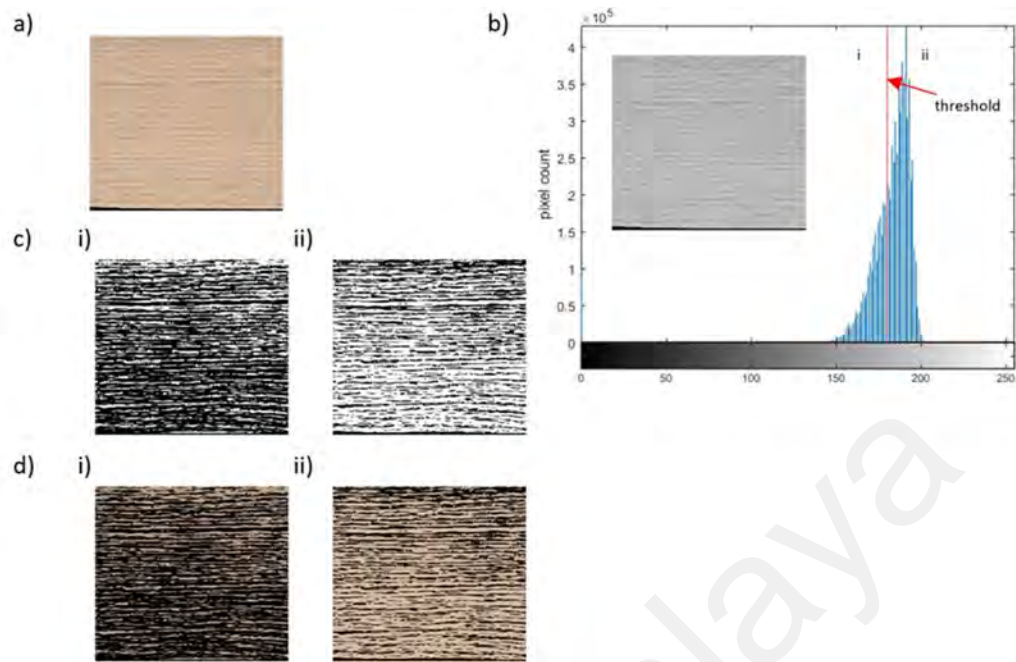
Figure 3.6 a) Pre-processed image. b) Thresholding of the grayscale histogram. c) i) Lower and ii) upper stratum bit mask. d) i) Lower and ii) upper stratum bit mask on the pre-processed image.

It is assumed that the bimodality of the plot to be present, though it may not be two equally normal plots as the example in Figure 3.6 b), typically or the species with less distinctive grains. After thresholding, the lower and upper strata bit masks were generated in Figure 3.6 c). The bit masks were then mapped onto the pre-processed colour image in Figure 3.6 a) to extract the colour layer in each stratum in Figure 3.6 d), where the means and standard deviations were estimated for each colour channel. Those values together with the Otsu threshold value were termed as the Otsu Soft Colour Descriptors (OCSDs). The OCSDs were extracted from each image in both full and half resolutions, and given corresponding notations, as tabulated in Table 3.3

Table 3.3 Notations for 26 OCSDs extracted from each image.

Soft Descriptor	Resolution	Lower Stratum, L			Upper Stratum, U		
			Notation				
Otsu Thresholding Value, OTV	**Full, F**		OTV_F				
	Half, H		OTV_H				
		R	**G**	**B**	**R**	**G**	**B**
Mean, μ	**Full, F**	μ_{FLR}	μ_{FLG}	μ_{FLB}	μ_{FUR}	μ_{FUG}	μ_{FUB}
	Half, H	μ_{HLR}	μ_{HLG}	μ_{HLB}	μ_{HUR}	μ_{HUG}	μ_{HUB}
Standard Deviation, σ	**Full, F**	σ_{FLR}	σ_{FLG}	σ_{FLB}	σ_{FUR}	σ_{FUG}	σ_{FUB}
	Half, H	σ_{HLR}	σ_{HLG}	σ_{HLB}	σ_{HUR}	σ_{HUG}	σ_{HUB}

3.2.3 Feature Selection

Feature selection is essential in reducing the dimensionality of the feature vector to minimize the computational efforts for real-life applications. This involves the identification of the contributing features in the classification, thus eliminating the redundant ones from the features set. The Sequential Forward Selection (SFS) is a well-known wrapper method in feature selection algorithms that trains a classifier model through iterative trials with different combinations of features. In this study, Linear Discriminant Analysis (LDA) was used as the classifier for its ease of implementation and relatively stable performance.

LDA is a supervised classifier which uses a feature vector (or data vector) of m-columns of features by n-rows of observations, each row with a known class label to find the linear discriminants that maximize the interclass distance. The following are the processing steps for LDA model training (Raschka, 2014; Tanner, 2021):

1. Calculate the class mean vectors, $\boldsymbol{m}_i = \begin{bmatrix} \mu_{i,1} \\ \mu_{i,2} \\ ... \\ \mu_{i,j} \end{bmatrix}$, where $\mu_{i,j}$ is mean of feature j of

   class i.

2. Compute the between- and within-class scatter matrices.

   Within-class scatter matrix, S_W $S_W = \sum_{i=1}^{c}(N_i - 1) * S_i$, where S_i is the scatter

   matrix of class i, N_i is the number of rows in data vector of class i, c is number of

   classes, and scatter matrix of each class, $S_i = \frac{1}{N_i-1}\sum_{r=1}^{N_i}(\boldsymbol{x}_{i,r} - \boldsymbol{m}_i)(\boldsymbol{x}_{i,r} - \boldsymbol{m}_i)^T$,

   where $\boldsymbol{x}_{i,r}$ is the row vector r of class i, $\boldsymbol{m}_i$ is the mean vector of class i, and N_i is

   the number of rows in data vector of class i.

   Between-class scatter matrix, $S_B = \sum_{i=1}^{c} N_i(\boldsymbol{m}_i - \boldsymbol{m})(\boldsymbol{m}_i - \boldsymbol{m})^T$, where $\boldsymbol{m}_i$ is

   the mean vector of class i, $\boldsymbol{m}$ is the overall mean vector, N_i is the number of rows

   in data vector of class i, and c is the number of classes.

3. Compute the eigenvectors and their corresponding eigenvalues by solving the

   equation: $S_W^{-1}S_B\boldsymbol{v} = \lambda\boldsymbol{v}$, where S_W is the within-class scatter matrix, S_B is the

   between-class scatter matrix, $\boldsymbol{v}$ is the eigenvector, and λ is the eigenvalue.

4. Sort eigenvalues in descending order and select the top k eigenvectors

   corresponding to the eigenvalues.

5. Construct the transformation matrix by arranging eigenvectors as columns.

To test evaluate the performance of the LDA model:

1. Transform the test set into new subspace with the transformation matrix.

2. Compare each data point with each and assign the colour group with the closest

   mean to it.

3. Calculate the accuracy by computing the percentage of correctly assigned data

   points.

SFS starts with an empty feature set. All the features will be tested individually to find the feature which gives the best classification results and add it to the feature set. Then, the remaining features will be paired with the winning feature to find the best combination. The process is repeated until the criterion is met, either certain size of the feature set or accuracy level is reached, or the classification result has reached a plateau where there is no significant improvement in the accuracy with increasing number of features. For this study, the stopping criterion is that the number of features used reaches ten.

Five-fold cross validation is used to determine the winning feature. This is done by splitting the dataset into five equivalent subsets, where four of the sets are used for LDA model training, and the remaining set is used as the test set. Five training and testing processes are performed with one subset being used as the testing set in each iteration respectively. The performance metric is obtained by averaging the classification accuracy of the five tests.

3.2.4 Classifier

Self-Organizing Map (SOM) was first proposed by Kohonen (1990), which uses the unsupervised machine learning technique to transform a high dimensional dataset into a more visualizable two-dimensional map, as exemplified in Figure 3.7. It is a type of artificial neural network but trained with competitive learning mechanism. The map is first initialized with m-rows by n-columns nodes of N-feature depth, each with a randomized weight value (also known as the seed value). Each data point will be tested with all the nodes to find the closest node (also known as best matching unit, or BMU) with the shortest Euclidean distance computed as shown in Equation (3.1). The weights of the node and its surrounding or neighbouring nodes are then updated as per Equation (3.4) to approach the data point at a certain training rate. The process is repeated for all

the data points, followed by multiple iterations with a decaying neighbourhood size as per Equation (3.2) and training rate as per Equation (3.3). In this study, a 6-row by 9-column hexagonal SOM map was used. The initial neighbourhood size, learning rate and the ordering of tuning phases are the default values by MATLAB: 3, 0.9, and 0.02 respectively. Varying number of epochs (2000, 12000, and 24000) were tested for both ordering and tuning parameters.
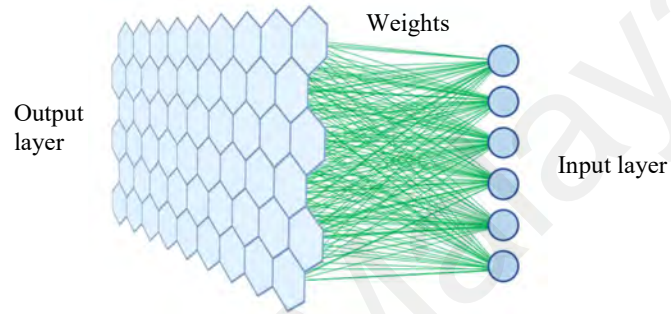
Figure 3.7 Graphical representation of SOM

$$D_{i,j} = \sqrt{\sum_{x=1}^{N} (W_{i,j,x} - W_x)^2} \qquad (3.1)$$

where

W_x weight of data for feature x

$W_{i,j,x}$ weight of node at column i and row j for feature x

$D_{i,j}$ distance between data and node (i,j)

N total number of features

$$H_t = H_0 \cdot e^{-t \cdot d_H} \qquad (3.2)$$

$$L_t = L_0 \cdot e^{-t \cdot d_L} \qquad (3.3)$$

$$W'_{i,j,x} = L_i \cdot e^{-\frac{r^2}{H_t}} \cdot \left(W_x - W_{i,j,x} \right) \qquad \textbf{(3.4)}$$

where

$W'_{i,j,x}$ new adjusted weight for feature x at node (i,j) at epoch t

H_0 neighbourhood rule

H_t neighbourhood rule at epoch t subjected to decay rate d_H

L_0 learning rate

L_t learning rate at epoch t subjected to decay rate d_L

r distance of node (i,j) from BMU node

Eventually, neighbouring nodes associated with more similar data points from the same group will form cluster, while different groups tend to cluster away from each other. The class of the node is determined by the simple majority rule from its associate data points. Each data point is pre-labelled with a class number, which depicts the colour group one is in. A node with no associated data points will be labelled as null, a node with all the data from the same class will be labelled as that class, while a node with data from more than one class will be classified to the class with highest count.

For testing, the weights (or the feature values) of an unknown sample are compared with the weights of only the labelled nodes, excluding the null ones. The closest node with the shortest Euclidean distance (or the BMU) calculated using the same Equation (3.1) is where the sample belongs, thus, it will be classified to the class of that node. The low computational cost and complexity of SOM makes it competent for deployments where speed is crucial.

In this study, the best features derived from SFS as well the full feature set were used in SOM training, and their performance were compared. The performance metric used is the misclassification count, assuming the human categorized colour groups to be true. Similarly, with the majority-wins rule, the node is classified to the colour group with the greatest number of data points from the same group, while the other data points from other group will be accumulated in the misclassification count. The conformance rates, complementary to misclassification rates were computed. This is iterated for different number of SOM epochs.

CHAPTER 4: RESULTS

In this chapter, the outcomes derived from the methodologies presented in the preceding chapter will be illustrated and examined through a series of figures and tables. The presentation aims to encapsulate the essence of the conducted experiments, providing a comprehensive understanding of the obtained results.

4.1   Calibration

The correlation between reference intensities from CE200 day 1 gamma adjusted calibration chart with intensities of all cameras is illustrated in Figure 4.1. Each correlation plot is constructed with 72 datapoints (24 reference colours by 3 colour channels R, G and B). The intensities of each colour channel range from 0 to 255 (8 bits per channel) for 24-bit image.

Figure 4.1 a) shows the correlation between gamma adjusted and raw intensities of CE200. It is a non-linear correlation, where the lower intensity values were boosted to a greater extent compared to the higher ones. Figure 4.1 b) compared the intensities of C920 with the adjusted intensities of CE200. The raw intensities of C920 in Figure 4.1 b) i) though were in a slight underexposure, showing a close correlation with the CE200 intensities after adjustment as shown in Figure 4.1 b) ii). RX0 II on the other hand was having an overexposure issue, where its intensities were flattened at 255 when the gamma adjusted values of CE200 exceeded value about 150, as shown in Figure 4.1 c) i). Although it showed better correlation with CE200 after adjustment in Figure 4.1 c) ii), but the plateaus remained noticeable. The overexposure could be the result of exposure compensation done internally by the RX0 II processor during image acquisition when there were dark regions of the lighting rim appeared in the field of view.

a)

b) i)

b) ii)

c) i)

c) ii)
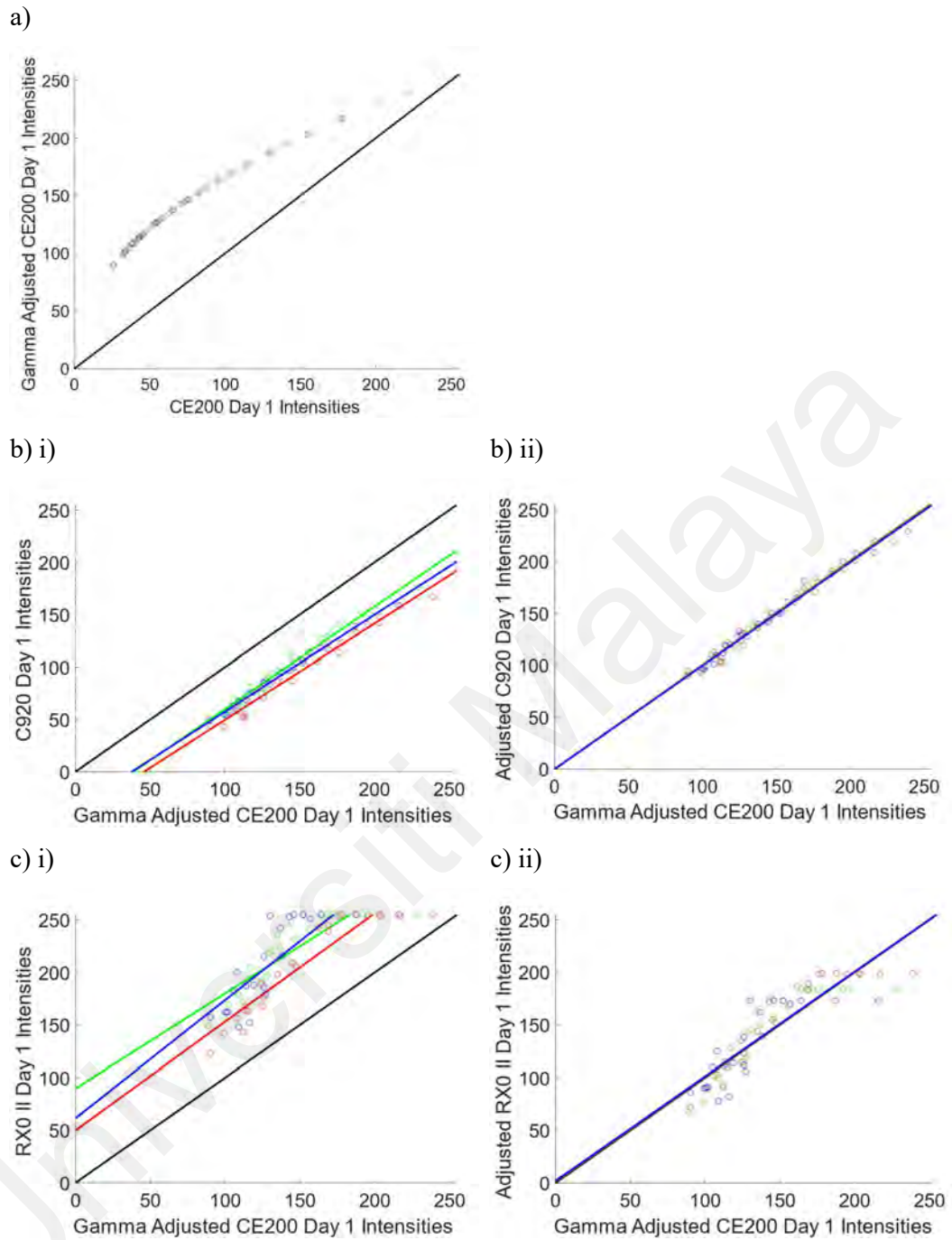
Figure 4.1 a) Correlation plot of CE200 Day 1 gamma adjusted against raw intensities. b), c) Correlation plots of C920, RX0 II Day 1 i) before and ii) after adjusted intensities against CE200 Day 1 gamma adjusted intensities.

Table 4.1 shows the percentage drifts within each camera between the calibration points on different days using the first day values as reference. The value 100% denotes negligible drift, the lower the value the larger the drift, the further away is it from the reference point. The drifts could be due to the use of different devices to connect to the cameras. For instance, a personal computer or laptop were used on different occasions. All three cameras were connected to the device via Universal Serial Bus (USB) cable for data transmission. CE200 and C920 were both powered by the same USB port each was connected to, whereas RX0 II was powered by its built-in rechargeable lithium-ion battery which loses charge while streaming data. C920 exhibited the most stable colour representations with minimal drifts for every session, while a relatively larger drift in CE200 was observed on the second day, calibration is therefore essential even with the industrial grade cameras for the unaccountable drifts as such.
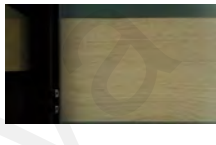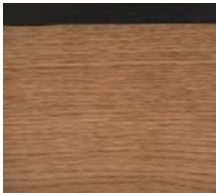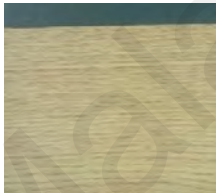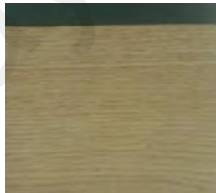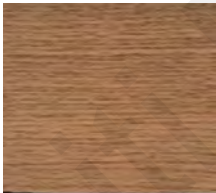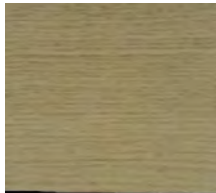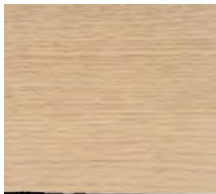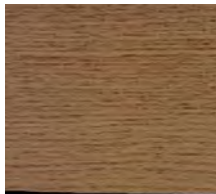
Table 4.1 ColorChecker calibration points' correlation plot percentage drift in R, G and B channel in each camera during each image acquisition session.

Date	CE200			C920			RX0 II		
	R	G	B	R	G	B	R	G	B
10/3/2022*	100.0	100.0	100.0	100.0	100.0	100.0	100.0	100.0	100.0
21/3/2022	82.1	99.5	83.7	99.7	99.7	100.0	99.9	100.0	100.0
31/3/2022	99.9	99.5	98.4	99.5	99.6	99.8	98.0	98.0	97.8
20/4/2022	99.5	98.7	97.6	100.0	100.0	100.0	99.2	99.2	99.3
28/4/2022	98.6	98.0	96.6	100.0	100.0	100.0	94.4	94.3	94.0
12/5/2022	97.6	97.9	96.9	100.0	100.0	100.0	97.2	97.3	97.2

* Calibration reference target

Table 4.2 shows the image preparation processes of a sample oak veneer images from the three cameras. The output images of CE200 and C920 showed a close resemblance in colour by inspection.

Table 4.2 Sample oak veneer image from each camera undergoing the image preparation processes.

Process	CE200	C920	RX0 II
Image Capturing			
Image Cropping			
Background Removal			
Colour Calibration*			

* CE200 images underwent an additional gamma correction process

4.2   Feature Performance

Figure 4.2 shows the individual feature performance plots of all three cameras in different species. CE200 and C920 had similar performance while RX0 II slightly underperformed.

Figure 4.2 The performance of 26 individual features in CE200, C920 and RX0 II for species a) red oak, b) yellow poplar and c) maple, the μ and σ features of each region are arranged orderly in R, G, B triplets.

It is observed that OTV_F outperformed OTV_H in most cases. These features represent the Otsu thresholding values, which separate the image grey histogram into lower and upper strata to isolate the grain from the basal part. Given that different colour groups exhibit varying distributions in both strata, particularly in the upper stratum, this threshold becomes a crucial indicator in colour classification. However, when the resolution is halved, performance diminishes. This dip may be attributed to unintended shifts in the threshold caused by averaging the brightness of adjacent pixels during the down-sampling. Overlapping thresholds make colour groups less distinguishable, causing the performance as such.

Generally, μ features performed better than σ features, suggesting that μ is a more distinguishable colour feature as an individual. Notably, μ_{FUG} stood out as the best individual feature. This aligns with the finding of Dowling and Dowling Jr (2016) on the human eye's sensitivity to green light. Meanwhile, upper stratum features μ_{FU} and μ_{HU} performed better than their lower stratum counterparts μ_{FL} and μ_{HL}, suggesting that the basal part of plays a more significant role than the grain part as colour descriptors. On the other hand, the feature performances from both resolutions are comparable, thus, processing images at half the original resolution may be recommended for systems where computational speed is crucial.

Figure 4.3 depicts the best performance values from five-fold cross-validation during SFS using LDA for each camera across all species. Stable performance for all cameras was observed from eight features onwards, SFS was therefore stopped at ten features, with an additional test with all 26 features for comparison. Notably, combination of features produced more convincing results than using single feature. It took around four features to reach optimal performance for both CE200 and C920. However, RX0 II required up to eight features, especially for maple. Interestingly, the use of all features

did not perform as well compared to the smaller feature sets, signifying the importance of feature selection as irrelevant features may hinder the classification performance.

a)

b)

c)
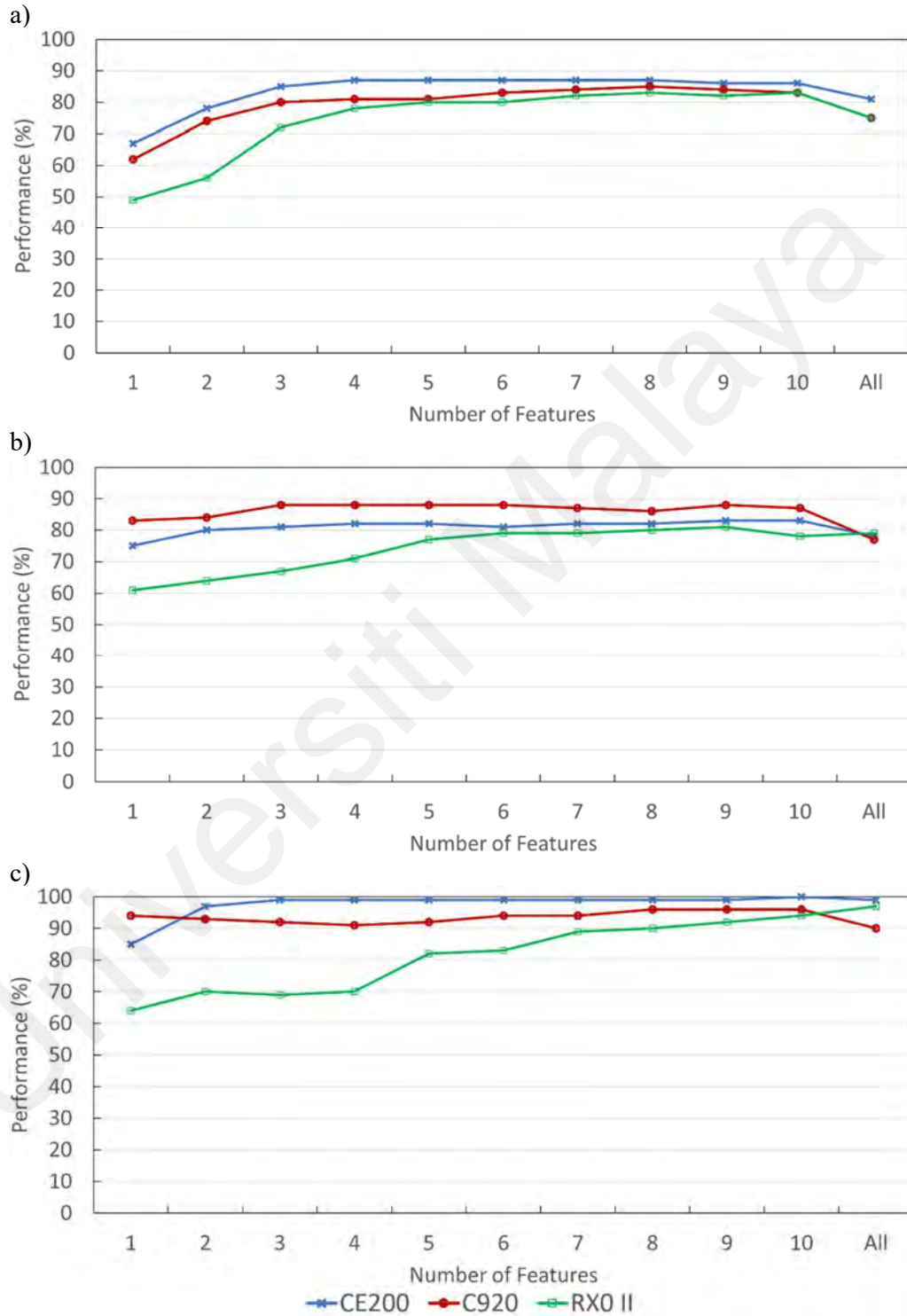
Figure 4.3 SFS performance of three cameras for a) red oak, b) yellow poplar and c) maple using the best scoring combinations of one to ten features as well as all features.

The top 5 ranking features derived from SFS for each camera in different species are shown in Table 4.3. μ_{FUG} being the dominant feature in all species, followed by μ_{FUR}. This conforms to the individual feature performance discussed earlier, where these two features outperformed most of the others individually, further enhancing the accuracy in a group with other features. Although the performance of μ_{FUB} surpassed μ_{FLB} as an individual in most cases, however, μ_{FLB} played a more significant role than μ_{FUB} in a group to achieve the best scoring feature set. This shows grain part feature (lower spectrum) though may not be as performing as basal part feature (upper stratum) when compared individually, it indeed contributes to the performance when combined with others. Overall, μ features are more favourable compared to σ features except for some occasions such as RX0 II in maple where the top 5 features were dominantly represented by σ values.

Table 4.3 Top 5 ranked features from SFS in each species for the three cameras*.

Rank	Red Oak			Yellow Poplar			Maple		
	CE200	**C920**	**RX0 II**	**CE200**	**C920**	**RX0 II**	**CE200**	**C920**	**RX0 II**
#1	μ_{FUG}	μ_{FUG}	μ_{HUB}	μ_{FUB}	μ_{FUG}	μ_{FLB}	μ_{FLB}	μ_{FUG}	σ_{FUB}
#2	μ_{FUR}	μ_{FUR}	μ_{HUG}	μ_{FUG}	μ_{HUB}	μ_{HLR}	μ_{FLG}	σ_{FLR}	σ_{FLB}
#3	μ_{FLB}	σ_{HUG}	μ_{FUR}	μ_{FLB}	μ_{HUG}	μ_{HLG}	OTV_H	μ_{FLG}	σ_{FLG}
#4	μ_{FLG}	μ_{FLR}	μ_{FLB}	σ_{FUB}	σ_{HUB}	μ_{HLB}	μ_{FLR}	σ_{FUB}	μ_{HLB}
#5	OTV_F	σ_{HLR}	OTV_F	σ_{FLB}	μ_{FLB}	μ_{FLR}	OTV_F	μ_{FUR}	μ_{HLG}

Confusion matrix visualised in Table 4.4 summarises the performance of top 5 SFS selected features for CE200. For red oak, there are some confusions between dark and orange groups as well as white and yellow. For yellow poplar, yellow is often confused with dark or white since it is a transition from dark to white. Maple has less confusions where all the groups are very well distinguishable. White generally is quite separable from darker colour like red and dark.

Table 4.4 Confusion matrix of different species for CE200 using LDA with top 5 SFS selected features, the columns are human categorized groups, the rows are SFS resulted groups.

Species		Colour Group* Confusion Matrix (Count)			
		D	**O**	**W**	**Y**
Red Oak	**D**	**154**	27	0	0
	O	6	**88**	0	1
	W	0	0	**83**	15
	Y	0	0	4	**137**
		D	**W**	**Y**	
Yellow Poplar	**D**	**91**	0	12	
	W	2	**118**	8	
	Y	22	9	**114**	
		R	**W**	**Y**	
Maple	**R**	**130**	4	0	
	W	0	**103**	0	
	Y	0	0	**161**	

* D = Dark, O = Orange, R = Red, W = White, Y = Yellow

Some colour groups are easily confused due to the ambiguous boundary between two adjacent colours in the wood colour spectrum. For example, white can be confused with yellow in red oak and yellow poplar, while dark is often mistaken as orange in red oak and yellow in yellow poplar. These colours overlap with each other in the spectrum that has no clear border line between colour bins. The darkest colour and the brightest colour on the other hand are mostly mutually exclusive, white in red oak and yellow poplar is having little to no confusion with dark group, and white in maple is well separable from red. These colours are usually further apart in the colour spectrum with minimal overlapping.

4.3   Classifier Performance

Figure 4.4 illustrated the performance of classifier SOM trained at different number of epochs (2000, 12000 and 24000) with naïve feature set and 2000 epochs with best feature set by SFS for all species and cameras. The conformation rate with the human-labelled groups was used as the performance metrics in this study. Interestingly, increasing the number of epochs had not improved the performance to a greater extent. On the contrary, in most cases where number of epochs increased from 2000 to 12000, declined conformation rates were recorded.
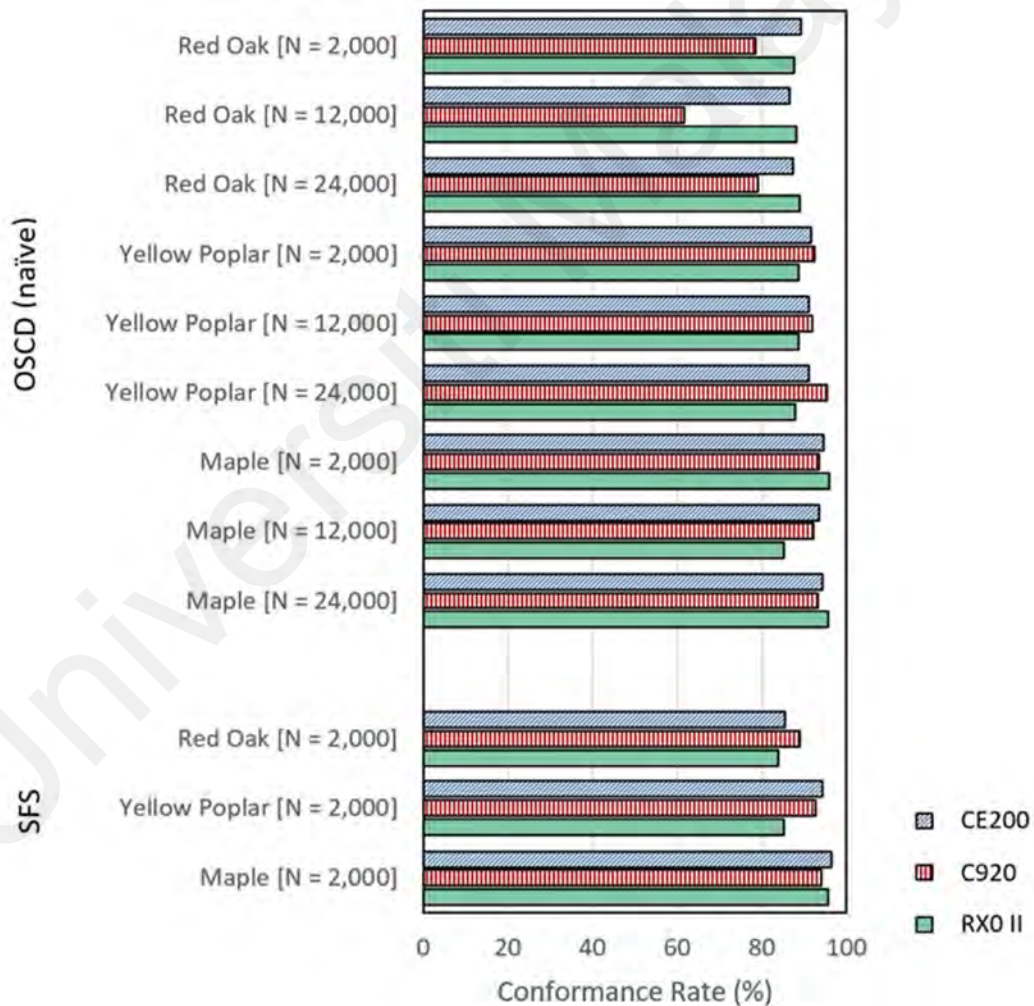

Figure 4.4 Performance of SOM based on conformation rate with human-labelled groups with naïve features at different number of epochs and SFS selected features at 2000 epochs for all species and devices.

On the other hand, the feature set with top five features that was selected by SFS with LDA and tested on SOM has outperformed the naïve set of all 26 features. The SFS selected features set has improved the performance of SOM, by having less computational efforts with smaller subset while showing higher accuracy. This technique can be implemented in industrial applications where high-speed decision making is required.

SOM is a clustering technique with no prior knowledge of the classes the data points belong. The schisms on the maps within the same cluster or colour group suggested that there could be an alternative way of categorizing the colours, for e.g., creating another subgroup. This could be another the scope in future studies. In this experiment setup, an overall conformation rates of 89.0 %, 94.5 % and 96.4 % were achieved for red oak, yellow poplar, and maple respectively.

During training, the number of datapoints from each class associated with each node were recorded. At the end of the training, each node is classified to the class having most datapoints according to the majority rule. For instance, the SOM map generated from the best performing species, maple with SFS selected features in Figure 4.5 shows the distribution of white, yellow, and red colour groups. White group highlighted in blue is the furthest away from the red group at the bottom, with yellow group between them. There is a node classified as white located in between the yellow and red regions, suggesting that there could be misaligned perceptions between human and the algorithm. The non-highlighted region is composed of the nodes with no datapoints falling into them during the training session, leaving them unlabelled. During actual implementation, this region will be ignored, only those labelled nodes will be considered in BMU evaluation.
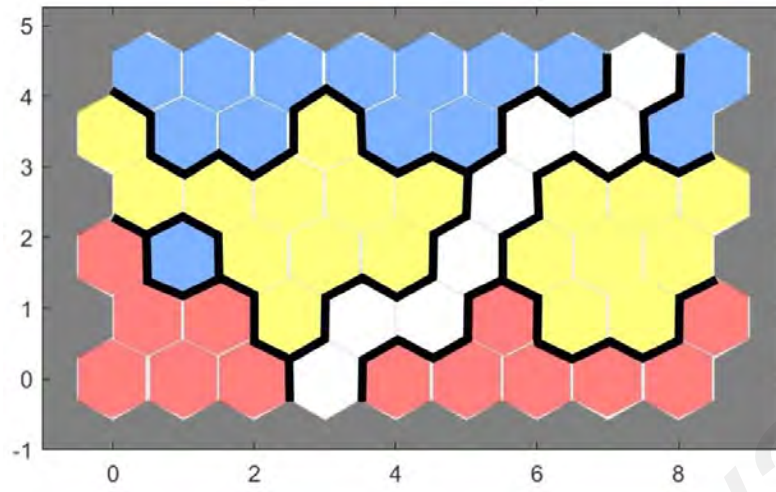
Figure 4.5 SOM map for maple for CE200 with selected features showing human categorized colour groups white, yellow, and red highlighted in blue, yellow, and red respectively.

CHAPTER 5: DISCUSSION

5.1 Camera Performance

The image acquisition software used for each device is different in this study. For instance, Machine Vision System (MVS) was used for CE200, MATLAB webcam image acquiring package for C920, and Sony Imaging Remote Software for RX0 II. Unlike MVS and MATLAB, where the parameters of the camera i.e., auto-white balance feature can be turned off, RX0 II had its auto-white balance turned on all the time. In addition to that, there could be some internal processing done automatically by the camera to beautify the image before outputting the images to the users, which is a common feature in most modern consumer cameras for aesthetic purposes. Therefore, the resulting calibration images showed different colour profiles from the reference image.

This study was limited by the access restriction to the camera parameters through the Imaging Remote Software. In future studies, Sony Camera Remote Software Development Kit (SDK) could be utilised for parameters adjustment. A custom connector may be required to connect the camera with personal computer for direct access to the SDK. The SDK would come in handy to control the camera settings such as exposure time, aperture size, auto-white balance, and post-processes handling. Alternatively, the presence of calibration chart in each image may be implemented for future studies for colour standardization, the results would be more representative for research purpose, though it may not be practical for industrial settings.

5.2   Comparison with Previous Studies

The proposed algorithm of this research has reported a conformation rate ranged from 89% to 96% for the species red oak, yellow poplar, and maple. This is analogous to SOM algorithm of Kurdthongmee (2008) on rubberwood (95% accuracy), fuzzy logic of Faria et al. (2008) on cherry, beech, and oak (over 95%), 1-NN classifier of Bianconi et al. (2013) on teak (90%) and SVM classifier of Nurthohari et al. (2019) on cedar (90%). It is noteworthy these studies were using sample size ranged from one to 30 each class. Some of them had produced more samples by using overlapping segments of the original images. Comparatively, this research has used nearly 100 different images per class per species. Furthermore, to account for intra-class variations, image acquisition was taken place on non-consecutive days. Therefore, the results from this study shall ensure greater reliability and robustness for real life applications.

The features selected by this study were mostly soft colour descriptors, particularly mean values and standard deviations in RGB colour space, were proven to be comparable to those of alternative colour spaces, for e.g., HSV or CIEL*a*b*. Bianconi's 1-NN classifier though different with SOM approach, but they are using similar comparators i.e., the Euclidean distance, thus their conclusion on different colour spaces complies with this study. On the other hand, the implementation of a fixed lighting condition and calibration to a reference date in this study was resemblance to the Bianconi's colour space transformation from RGB to CIEL*a*b*, the practical significance of colour space conversion remains debatable (Bianconi et al., 2013).

The difference between this study and most studies is the spectrum from which the descriptors were extracted. Generally, the conventional way of retrieving the means and standard deviations is by the whole image or a segmented window where all the pixels in the region will be evaluated to produce one set of descriptors, that is, single mean and

standard deviation value per channel. This study differed by performing Otsu thresholding on the grayscale image to isolate the grain from the basal part, hence harvesting two sets of descriptors from both spectra of different intensity levels. Thus, the characterisation of the wood colour is more comprehensive for a prominent result.

5.3   Industrial Implementation

The vision system developed in this study were deployed in WM's facility. While this study focused on red oak, yellow poplar and maple, several other veneer species were also tested for usability, namely red meranti (*Shorea* spp.), American white oak, American black walnut (*Juglans nigra*). While the other trained species trained were tested alright by the operators, it was found that performance for black walnut was not stable. This is because the timber contained many 'layers' of colour, which a single Otsu bifurcation into two intensity layers was insufficient to distinguish the different colour groups correctly as compared to human judgement. One possible solution would be to use multiple iterative Otsu thresholding to further extract more refined colour features of each colour layer.

Also, the same algorithm (and software) is being used with another industrial implementation at a separate facility, Sim Seng Huat Wood Industries Sdn. Bhd. (SSH) for performing colour sorting of light red meranti (*Shorea* spp.) solid timber (not veneers). Although the system setup in SSH uses line scan cameras with line lights, the same colour sorting algorithm is applicable. The system is flexible to allow user to train new species or train the existing species with more colour groups. The user-interface of the colour sorting software in Figure 5.1 showed that different species can be setup for training, and the parameters can also be changed for testing. For instance, while 9 × 6 SOM map was used in this study, a 12 × 9 map can be selected for a wider range of colours.
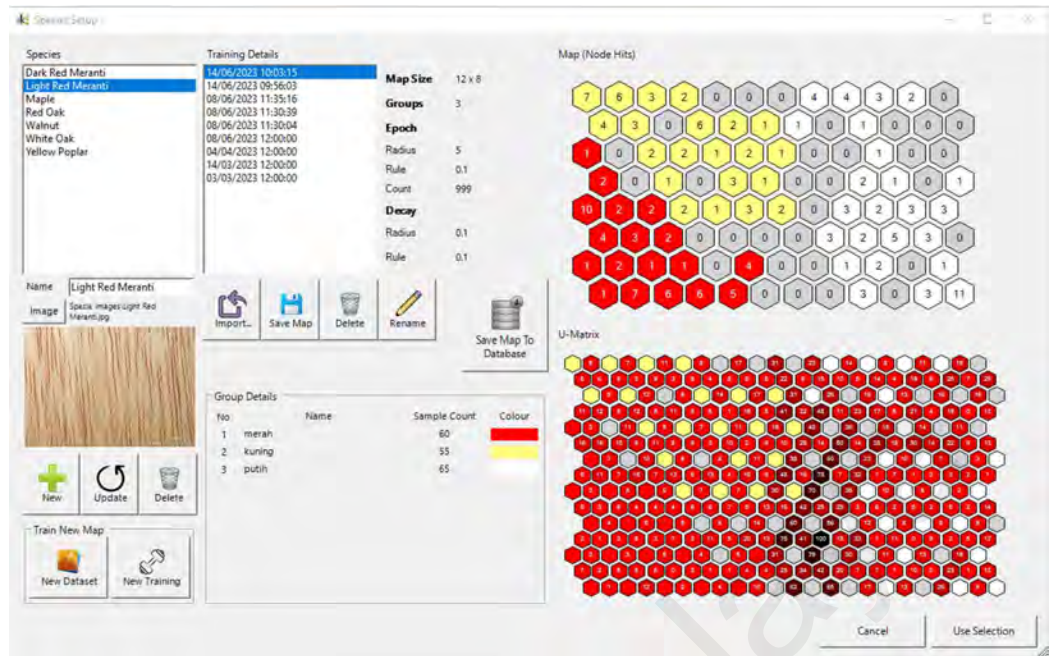
Figure 5.1 User-interface of colour sorting software deployed in WM with light red meranti selected.

CHAPTER 6: CONCLUSION

Among the cameras in this study, CE200 from Hikrobot has outperformed the rest, proving its viability as an industrial grade device. Interestingly, the second-best performing webcam C920 from Logitech had achieved an accuracy close to that of CE200. The results of RX0 II from Sony is the worst due to the software-related limitations mentioned earlier. Nevertheless, its performance may be improved if the camera settings are manually optimized. Therefore, a properly calibrated high-quality webcam could be an acceptable alternative when budget is of concern. However, the durability and other considerations in the industrial environment has yet to be tested.

This study confirmed that Otsu thresholding is feasible of separating the intensity levels of the grayscale wood images into lower and upper strata to represent the darker grain part and the brighter basal part respectively. The soft descriptors extracted from the higher stratum contributed significantly to the segregation of colour groups. The mean colour values from the basal part generally outperformed the other descriptors. Additionally, SFS approach is proven to enhance the sorting performance by selecting best performing features from the naïve feature set which may contain irrelevant features. On top of that, SOM is a robust classifier to sort the different colour groups for red oak, yellow poplar, and maple.

The system is currently being implemented in the industry for red oak, white oak, yellow poplar, maple and light red meranti. Performance for the black walnut was unsatisfactory and shall be scope in future studies.

REFERENCES

Annual Report. (2023). Malaysian Timber Industry Board. Retrieved August 5 from https://www.mtib.gov.my/en/annual-report

Bianconi, F., Fernández, A., González, E., & Saetta, S. A. (2013). Performance analysis of colour descriptors for parquet sorting. *Expert systems with applications*, *40*(5), 1636-1644.

Bombardier, V., & Schmitt, E. (2010). Fuzzy rule classifier: Capability for generalization in wood color recognition. *Engineering Applications of Artificial Intelligence*, *23*(6), 978-988.

Bombardier, V., Schmitt, E., & Charpentier, P. (2008). Color sorting system by fuzzy sensor. *TRAITEMENT DU SIGNAL*, *25*(5), 381-400.

Buehlmann, U., & Thomas, R. E. (2002). Impact of human error on lumber yield in rough mills. *Robotics and Computer-Integrated Manufacturing*, *18*(3-4), 197-203.

Coefficient of Kurtosis. Retrieved December 20 from https://grapherhelp.goldensoftware.com/WTOPICS/WKS_Kurtosis.htm

Color Management: Know about Color Spaces. Retrieved December 20 from https://www.linshangtech.com/tech/color-space-tech1439.html

Dome Lights. Retrieved December 12 from https://www.keyence.com.my/ss/products/vision/peripheral/ca-d/ca_dd.jsp

Dowling, J. E., & Dowling Jr, J. L. (2016). *Vision: How it works and what can go wrong*. MIT Press.

Eshaq, R. M. A., Hu, E., Li, M., & Alfarzaeai, M. S. (2020). Separation between coal and gangue based on infrared radiation and visual extraction of the YCbCr color space. *IEEE Access*, *8*, 55204-55220.

Faria, J., Martins, T., Ferreira, M., & Santos, C. (2008). A computer vision system for color grading wood boards using fuzzy logic. 2008 IEEE International Symposium on Industrial Electronics,

File:Color solid comparison hsl hsv cube cylinder cone.png. Retrieved December 20 from https://en.wikipedia.org/wiki/File:Color_solid_comparison_hsl_hsv_cube_cylinder_cone.png

File:YCbCrColorSpace Perspective.png. Retrieved December 20 from https://en.wikipedia.org/wiki/File:YCbCrColorSpace_Perspective.png

Heffernan, W., Frater, L., & Watson, N. (2007). LED replacement for fluorescent tube lighting. 2007 Australasian Universities Power Engineering Conference,

Hiremath, P. S., & Bhusnurmath, R. A. (2016). Industrial applications of colour texture classification based on anisotropic diffusion. International Conference on Recent Trends in Image Processing and Pattern Recognition,

Hiremath, P. S., & Bhusnurmath, R. A. (2017). Multiresolution LDBP descriptors for texture classification using anisotropic diffusion with an application to wood texture analysis. *Pattern Recognition Letters*, *89*, 8-17.

Høibø, O., & Nyrud, A. Q. (2010). Consumer perception of wood surfaces: the relationship between stated preferences and visual homogeneity. *Journal of wood science*, *56*(4), 276-283.

How to Convert an RGB Image to a Grayscale. https://www.baeldung.com/cs/convert-rgb-to-grayscale

Hu, X. Y., Wang, P. L., & Xu, J. Y. (2013). A wood color classifier based on CAV and SVM. Applied Mechanics and Materials,

Jonsson, O., Lindberg, S., Roos, A., Hugosson, M., & Lindström, M. (2008). Consumer perceptions and preferences on solid wood, wood-based panels, and composites: A repertory grid study. *Wood and Fiber Science*, 663-678.

Kashyapa, R. (2021). *Area Scan vs Line Scan: What Fits You Better?* Retrieved December, 12 from https://qualitastech.com/image-acquisition/area-scan-vs-line-scan-cameras/

Kavitha, J., & Suruliandi, A. (2018). Feature extraction using dominant local texture-color patterns (DLTCP) and classification of color images. *Journal of medical systems*, *42*(11), 1-12.

Khan, Z., Yang, J., & Zheng, Y. (2019). Efficient clustering approach for adaptive unsupervised colour image segmentation. *IET Image Processing*, *13*(10), 1763-1772.

Kohonen, T. (1990). The self-organizing map. *Proceedings of the IEEE*, *78*(9), 1464-1480.

Kuhn, M., & Johnson, K. (2013). *Applied predictive modeling* (Vol. 26). Springer.

Kurdthongmee, W. (2008). Colour classification of rubberwood boards for fingerjoint manufacturing using a SOM neural network and image processing. *Computers and electronics in agriculture*, *64*(2), 85-92.

Lin, Y., Chen, D., Liang, S., Xu, Z., Qiu, Y., Zhang, J., & Liu, X. (2020). Color Classification of Wooden Boards Based on Machine Vision and the Clustering Algorithm. *Applied Sciences*, *10*(19), 6816.

Line Scan Cameras vs Area Scan Cameras – Which Is Suitable For Your Applications? https://www.voltrium.com.sg/en/line-scan-cameras-vs-area-scan-cameras/

Liu, J., & Furuno, T. (2002). The fractal estimation of wood color variation by the triangular prism surface area method. *Wood Science and Technology*, *36*(5), 385-397.

Liu, S., Jiang, W., Wu, L., Wen, H., Liu, M., & Wang, Y. (2020). Real-time classification of rubber wood boards using an SSR-based CNN. *IEEE Transactions on Instrumentation and Measurement*, *69*(11), 8725-8734.

Lu, Q., Srikanteswara, S., King, W., Drayer, T., Conners, R., Kline, E., & Araman, P. (1997). Machine vision system for color sorting wood edge-glued panel parts. Proceedings of the IECON'97 23rd International Conference on Industrial Electronics, Control, and Instrumentation (Cat. No. 97CH36066),

Lu, W., & Tan, J. (2004). Grain pattern characterization and classification of walnut by image processing. *Wood and Fiber Science*, *36*(3), 311-318.

Malaysia External Trade Statistics. (2022, October 19). Department of Statistics Malaysia. Retrieved August 5 from https://www.dosm.gov.my/portal-main/release-content/malaysia-external-trade-statistics-bulletin-september-2022

Manjunath, B. S., Ohm, J.-R., Vasudevan, V. V., & Yamada, A. (2001). Color and texture descriptors. *IEEE Transactions on circuits and systems for video technology*, *11*(6), 703-715.

McCamy, C. S., Marcus, H., & Davidson, J. G. (1976). A color-rendition chart. *J. App. Photog. Eng*, *2*(3), 95-99.

Monochrome Camera vs. Color Camera: All You Need to Know. Retrieved December 20 from https://www.technexion.com/resources/monochrome-camera-vs-color-camera-all-you-need-to-know/

Musat, E.-C., Salca, E.-A., Dinulica, F., Ciobanu, V. D., & Dumitrascu, A.-E. (2016). Evaluation of color variability of oak veneers for sorting. *BioResources*, *11*(1), 573-584.

Naqvi, S. A. A. (1996). Critical human factor issues in quality inspection tasks. *Journal of King Saud University-Engineering Sciences*, *8*(1), 133-140.

Nurthohari, Z., Murti, M. A., & Setianingsih, C. (2019). Wood Quality Classification Based on Texture and Fiber Pattern Recognition using HOG Feature and SVM Classifier. 2019 IEEE International Conference on Internet of Things and Intelligence System (IoTaIS),

Perdahci, C., Akin, H., & Cekic, O. (2018). A comparative study of fluorescent and LED lighting in industrial facilities. IOP Conference Series: Earth and Environmental Science,

Ramesh, G., Siddhartha, T., Sivaraman, K., & Subramani, V. (2021). Identification of Timber Defects Using Convolution Neural Network. 2021 6th International Conference on Communication and Electronics Systems (ICCES),

Raschka, S. (2014). *Linear Discriminant Analysis*. Retrieved August 27 from https://sebastianraschka.com/Articles/2014_python_lda.html

Ratnasingam, J., Ab Latib, H., Yi, L. Y., Liat, L. C., & Khoo, A. (2019). Extent of automation and the readiness for industry 4.0 among Malaysian furniture manufacturers. *BioResources*, *14*(3), 7095-7110.

Rozman, D., Brezak, M., & Petrovic, I. (2006). Parquet sorting and grading based on color and texture analyses. 2006 IEEE International Symposium on Industrial Electronics,

Singh, C., Walia, E., & Kaur, K. P. (2018). Color texture description with novel local binary patterns for effective image retrieval. *Pattern recognition*, *76*, 50-68.

SIRIM. (2021). *SIRIM, MTIB to Revolutionise Local Timber Industry, Explore Solar Energy for Kiln Drying of Timber* https://www.sirim.my/Pages/SIRIM-Press-Release/SIRIM-MTIB-MOU.aspx

Skew. Retrieved December 20 from https://www.biologyforlife.com/skew.html

Sosef, M. S. M. (2017). *Shorea stenoptera (PROSEA)*. Retrieved August 22 from https://uses.plantnet-project.org/en/Shorea_stenoptera_(PROSEA)

Srikanteswara, S., Lu, Q. O., King, W., Drayer, T. H., Conners, R. W., Kline, D. E., & Araman, P. A. (1997). Real-time implementation of a color sorting system. Machine Vision Applications, Architectures, and Systems Integration VI,

Sunoj, S., Igathinathane, C., Saliendra, N., Hendrickson, J., & Archer, D. (2018). Color calibration of digital images for agriculture and other applications. *ISPRS journal of photogrammetry and remote sensing*, *146*, 221-234.

Tanner, G. (2021). *Linear Discriminant Analysis (LDA)*. Retrieved August 22 from https://ml-explained.com/blog/linear-discriminant-analysis-explained

Wang, Z., Zhuang, Z., Liu, Y., Ding, F., & Tang, M. (2021). Color Classification and Texture Recognition System of Solid Wood Panels. *Forests*, *12*(9), 1154.

Wood Products. (2021). The Observatory of Economic Complexity. Retrieved August 5 from https://oec.world/en/profile/hs/wood-products

Zhang, Z., Zhao, M., Li, B., Tang, P., & Li, F.-Z. (2015). Simple yet effective color principal and discriminant feature extraction for representing and recognizing color images. *Neurocomputing*, *149*, 1058-1073.

Zhuang, Z., Liu, Y., Ding, F., & Wang, Z. (2021). Online Color Classification System of Solid Wood Flooring Based on Characteristic Features. *Sensors*, *21*(2), 336.